ASD TECHNICAL REPORT 61-11
VOLUME II

SOLAR CELL ARRAY OPTIMIZATION

(VOLUME II)

TECHNICAL REPORT No. ASD TR 61-11

FEBRUARY 1962

FLIGHT ACCESSORIES LABORATORY
AERONAUTICAL SYSTEMS DIVISION
AIR FORCE SYSTEMS COMMAND
WRIGHT-PATTERSON AIR FORCE BASE, OHIO

PROJECT No. 3145, TASK No. 60959

(Prepared under Contract No. AF 33(616)-7415
by Astro-Electronics Division, Defense Electronic Products,
Radio Corporation of America, Princeton, N. J.)

NOTICES

When Government drawings, specifications, or other data are used for any purpose other than in connection with a definitely related Government procurement operation, the United States Government thereby incurs no responsibility nor any obligation whatsoever; and the fact that the Government may have formulated, furnished, or in any way supplied the said drawings, specifications, or other data, is not to be regarded by implication or otherwise as in any manner licensing the holder or any other person or corporation, or conveying any rights or permission to manufacture, use, or sell any patented invention that may in any way be related thereto.

Qualified requesters may obtain copies of this report from the Armed Services Technical Information Agency, (ASTIA), Arlington Hall Station, Arlington 12, Virginia.

This report has been released to the Office of Technical Services, U. S. Department of Commerce, Washington 25, D. C., for sale to the general public.

Copies of ASD Technical Reports and Technical Notes should not be returned to the Aeronautical Systems Division unless return is required by security considerations, contractual obligations, or notice on a specific document.

200 - April 1962 - 28-1211 & 1212

Aeronautical Systems Division, Wright-Patterson Air Force Base, Ohio. Rpt No. ASD-TR-61-11, Vol. II. SOLAR CELL ARRAY OPTIMIZATION. Feb 62, 85p, incl. illus; tables.

Unclassified Report

This report covers the fabrication and test of photovoltaic materials and design of solar-cell arrays for maximum conversion of solar energy with minimum weight. Evaporated layer cells with an efficiency of up to 4.5 percent over an area of 1.6 cm^2 were fabricated. Research on crystal layer conversion reduced the temperature for recrystallization from 500°C to 300°C. Two

(over)

models of solar-cell arrays to simulate a 100 ft^2 system were fabricated: the telescoping sail with a density of 0.075 lb/ft^2, and the inflatable torus sail with a density of 0.04 lb/ft^2. The maximum area of individual cells was increased by a factor of 27, thickness of substrate reduced by factor of 6, and weight reduced by factor of 7.

1. Solar Cells
2. Photovoltaic materials
3. Solar Energy Conversion

I. ASD Project 3145, Task 60959

II. Contract AF33(616)-7415

III. RCA, Astro-Electronics Div., Defense Electronic Products, Princeton, N. J.

IV. In ASTIA collection

V. Avail fr OTS:

Aeronautical Systems Division, Wright-Patterson Air Force Base, Ohio. Rpt No. ASD-TR-61-11, Vol. II. SOLAR CELL ARRAY OPTIMIZATION. Feb 62, 85p, incl. illus; tables.

Unclassified Report

This report covers the fabrication and test of photovoltaic materials and design of solar-cell arrays for maximum conversion of solar energy with minimum weight. Evaporated layer cells with an efficiency of up to 4.5 percent over an area of 1.6 cm^2 were fabricated. Research on crystal layer conversion reduced the temperature for recrystallization from 500°C to 300°C. Two

(over)

models of solar-cell arrays to simulate a 100 ft^2 system were fabricated: the telescoping sail with a density of 0.075 lb/ft^2, and the inflatable torus sail with a density of 0.04 lb/ft^2. The maximum area of individual cells was increased by a factor of 27, thickness of substrate reduced by factor of 6, and weight reduced by factor of 7.

1. Solar Cells
2. Photovoltaic materials
3. Solar Energy Conversion

I. ASD Project 3145, Task 60959

II. Contract AF33(616)-7415

III. RCA, Astro-Electronics Div., Defense Electronic Products, Princeton, N. J.

IV. In ASTIA collection

V. Avail fr OTS:

Aeronautical Systems Division, Wright-Patterson Air Force Base, Ohio. Rpt No. ASD-TR-61-11, Vol. II. SOLAR CELL ARRAY OPTIMIZATION. Feb 62, 85p, incl. illus; tables.

Unclassified Report

This report covers the fabrication and test of photovoltaic materials and design of solar-cell arrays for maximum conversion of solar energy with minimum weight. Evaporated layer cells with an efficiency of up to 4.5 percent over an area of 1.6 cm^2 were fabricated. Research on crystal layer conversion reduced the temperature for recrystallization from 500°C to 300°C. Two

(over)

models of solar-cell arrays to simulate a 100 ft^2 system were fabricated: the telescoping sail with a density of 0.075 lb/ft^2, and the inflatable torus sail with a density of 0.04 lb/ft^2. The maximum area of individual cells was increased by a factor of 27, thickness of substrate reduced by factor of 6, and weight reduced by factor of 7.

1. Solar Cells
2. Photovoltaic materials
3. Solar Energy Conversion

I. ASD Project 3145, Task 60959

II. Contract AF33(616)-7415

III. RCA, Astro-Electronics Div., Defense Electronic Products, Princeton, N. J.

IV. In ASTIA collection

V. Avail fr OTS:

Aeronautical Systems Division, Wright-Patterson Air Force Base, Ohio. Rpt No. ASD-TR-61-11, Vol. II. SOLAR CELL ARRAY OPTIMIZATION. Feb 62, 85p, incl. illus; tables.

Unclassified Report

This report covers the fabrication and test of photovoltaic materials and design of solar-cell arrays for maximum conversion of solar energy with minimum weight. Evaporated layer cells with an efficiency of up to 4.5 percent over an area of 1.6 cm^2 were fabricated. Research on crystal layer conversion reduced the temperature for recrystallization from 500°C to 300°C. Two

(over)

models of solar-cell arrays to simulate a 100 ft^2 system were fabricated: the telescoping sail with a density of 0.075 lb/ft^2, and the inflatable torus sail with a density of 0.04 lb/ft^2. The maximum area of individual cells was increased by a factor of 27, thickness of substrate reduced by factor of 6, and weight reduced by factor of 7.

1. Solar Cells
2. Photovoltaic materials
3. Solar Energy Conversion

I. ASD Project 3145, Task 60959

II. Contract AF33(616)-7415

III. RCA, Astro-Electronics Div., Defense Electronic Products, Princeton, N. J.

IV. In ASTIA collection

V. Avail fr OTS:

FOREWORD

This report was prepared by the Astro-Electronics Division of RCA on Air Force Contract No. AF 33(616) 7415 and Task No. 60959 of Project No. 0(3-3145), "Research and Development Program Involving Solar Cell Array Optimization." The report describes work performed from March 1961 through October 1961. In the performance of this work, the Astro-Electronics Division has been assisted by personnel of RCA Laboratories.

The work was administered under the direction of the Flight Accessories Laboratory of Aeronautical Systems Division. Mr. P. R. Bertheaud was task engineer for the Laboratory.

This report, Volume II, is the second progress report on the solar cell array program. (The initial report, the Summary Technical Report published August 1961, was not designated Volume I.)

ABSTRACT

This interim technical report presents the results of the fabrication and test phase of Contract No. AF 33(616) 7415. The overall objective of the work under this contract is to obtain the maximum electrical power conversion of solar energy in space per unit of system weight.

The phase of the work described by this report has had a two-fold objective:

(1) The continuation of research on photovoltaic materials in the form of polycrystalline evaporated layers, and studies on the possibility of recrystallizing certain of these thin layers.

(2) The fabrication both of a number of cadmium sulfide thin-film cells and of models of two oriented solar-cell arrays.

Research on photovoltaic materials has resulted in the fabrication of evaporated layer cells with an efficiency of up to 4.5 percent over an area of 1.6 cm^2. Research on crystal-layer conversion has resulted in a substantial reduction of the temperature required for recrystallization from 500° C to 300° C, with activation by either silver or copper.

Two demonstration models of arrays designed for least weight-to-area ratio were fabricated and are described. One of the arrays, the telescoping sail, simulates a space system which with a 100 ft^2 area would have a density without cells of 0.075 lb/ft^2. The other array, the inflatable torus sail, simulates a 100 ft^2 system that would have a density of less than 0.04 lb/ft^2.

About 120 CdS cells with an active area of 300 cm^2 were fabricated and are described. These cells represent a total power output of 500 milliwatts as initially measured. During the work described in this report the maximum area of individual cells was increased by a factor of 27 (to 44 cm^2), the thickness of substrate was reduced by a factor of 6 (to 0.010") and weight was reduced by a factor of 7 (to .068 gm/cm^2).

TABLE OF CONTENTS

TABLE OF CONTENTS (Cont.)

(Note - A materials section has been prepared in accordance with Table LXXV as a separate Materials Report dated October 1961 and published as required by Item VI of the contract.)

LIST OF ILLUSTRATIONS

LIST OF ILLUSTRATIONS (Cont.)

LIST OF TABLES

INTRODUCTION

The work described in this report covers the fabrication phase of the contract and continued research for the improvement of thin-film, large area, photovoltaic cells. The research has been concerned primarily with photovoltaic materials and crystal layer conversion. Detailed descriptions of this work are given in Sections I and II. Some work on fabrication of cells was included in the materials research but the objective of that fabrication was only to permit evaluation of various materials. The cells that were fabricated on a semi-production basis for delivery to ASD are described in Section III. The two array structures that were fabricated for delivery to ASD are the inflatable torus sail array and the telescoping array. The fabrication of these structures is described in Section IV.

The programs of attaching the CdS cells to the torus sail and of environmental testing of the completed arrays, which were planned originally, were cancelled during the latter stages of the work by mutual RCA-ASD agreement (see Section V).

The use of thin-film, large-area, photovoltaic cells offers the promise of obtaining solar sources with power output per pound greater than that of sources currently in use. The effort during this phase of work has resulted in the fabrication of two model solar arrays that simulate space arrays visualized for maximum power output per system weight consistent with maximum reliability and minimum pre-launch volume. Fabrication of the CdS cells has indicated the problems encountered in small scale manufacture but has also provided encouragement for the possibility of significant improvements. Further research work and continued improvement will constitute a major step toward the reduction of weight in future solar power systems, and should thus be a significant contribution to the country's space program.

Manuscript released by the authors October 1961 for publication as an ASD Technical Report.

TECHNICAL DISCUSSION

I. PHOTOVOLTAIC MATERIALS

INTRODUCTION

The discussion of photovoltaic materials in the preceding Summary Technical Report described factors involved in the fabrication of a polycrystalline CdS thin-film photovoltaic cell. At that time, the best cells exhibited conversion efficiencies of between 2 and 3 percent and had active areas of about 1.3 cm^2. To make these cells, polycrystalline CdS films having thicknesses up to 10 microns were formed by the vacuum evaporation of CdS powder or pellets onto heated transparent conducting Pyrex substrates. Photovoltaic cells were fabricated from these films by applying to the exposed CdS surface a thin layer of copper paint, consisting of finely divided copper suspended in a lacquer vehicle. The copper paint was allowed to dry in air. Cell fabrication was completed by heating the cell to 300°C in argon during a 10-minute period. This barrier formation process was not reproducible, and hence neither were the cell efficiencies.

A factor which limited cell efficiency is the relatively high resistance of the transparent electrode. This was particularly noticeable with cells having active areas greater than about 5 cm^2.

Preliminary measurements indicated that exposure to the atmosphere causes a deterioration of cell output. The deterioration can be reduced by enclosing the cell in an inert atmosphere or vacuum.

Since the writing of the last Summary Technical Report work on the CdS thin-film photovoltaic cell has been concerned with the following topics:

a. barrier formation,

b. cell fabrication,

c. testing of cells,

d. cell deterioration,

e. large area cells,

f. radiation damage,

g. thin substrates.

The main objectives of this work have been to increase the conversion efficiency and to increase the active area of the CdS cells.

TECHNICAL DISCUSSION

1. BARRIER FORMATION

Previous work on the evaporated CdS thin-film cells indicated that the efficiency of the completed cell was somehow related to the degree of darkening which appeared after processing at the interface between the CdS film and the copper contact; the darker the interface, the more efficient the cell. This observation was pointed out in the last Summary Technical Report but had not been investigated at that time.

A number of experiments were performed, and it soon became apparent that the interfacial darkening described above could easily be achieved by applying the copper paint to the CdS film and then heating the film in air to about 70°C for approximately one-half hour, while taking care not to allow the solvent of the copper paint to evaporate. The solvent evaporation could be retarded by simply placing a piece of non-porous paper (glassine paper) over the copper paint and applying a small amount of pressure to the CdS-copper paint-paper arrangement. When this method was used, the copper paint remained soft and flowing during the 70° C heat treatment. After the interface was of sufficient darkness, as determined by eye, the non-porous paper was removed and a small amount of additional copper paint was applied to the CdS film to provide an opaque covering over the entire surface. This copper paint layer was allowed to dry in air at room temperature. The cell was subsequently heated to 300°C in an argon atmosphere in as short a time as possible, usually four minutes; if the heating time exceeded 10 minutes, cell efficiency was sacrificed. The cell was then cooled rapidly in the argon atmosphere. The careful removal of the copper paint with a suitable solvent, and the contacting of the darkened region of the CdS film with either an air-drying silver paint or an evaporated silver layer completed cell fabrication, with the exception of a final step.

Metallic contact to the darkened surface of the CdS film was applied in such a manner as to leave a small area around the periphery of the CdS film uncontacted. At first this was done because of the difficulty of contacting the entire CdS darkened surface without shorting the darkened surface and the transparent tin-oxide electrode. However, the shape of the current-voltage curves indicated that shorting was occurring in spite of this precaution. The nature of the CdS vacuum evaporation, in which a mask is used to control the shape and position of the deposit, causes a shadowing effect to occur. The result

of this shadowing effect is to produce a deposit at the edge of the CdS film; the deposit is wedge-shaped when viewed in cross-section. The thin portion of this wedge permits a certain amount of shorting to occur between the darkened surface of the CdS film and the tin oxide electrode. It was found necessary, therefore, to remove a small area around the periphery of the CdS film to obtain maximum conversion efficiency. Edge removal was accomplished by carefully scraping the periphery of the CdS film with a razor blade. The effect of removing the edge of one cell was to increase the open-circuit voltage, short-circuit current, and efficiency by 5 percent, 7 percent and 37 percent, respectively. The shape of the current-voltage curve indicated that a higher shunt resistance was present.

The procedure described above for the formation of the barrier layer was difficult to control with respect to time and temperature. In addition, the solvent evaporated slowly, even with the precaution described above. A new approach was devised and is the procedure in use at present. A Pyrex tube, approximately 1-1/2 inches in diameter and twelve inches long, with one end sealed off, was placed in a small furnace with its length vertical and the sealed end downward, so that the bottom three inches could be heated. About two inches of copper paint was placed in the tube. By using this arrangement, the temperature of the copper paint could be controlled easily, and the cool upper portion of the tube served to condense any solvent that evaporated. The substrate upon which the CdS film was deposited was inserted or dipped into the copper paint by means of a long holder, and was agitated periodically to provide mixing of the copper paint. This procedure produces a more uniform darkening of the surface of the individual CdS films and was much easier to apply. When the film was removed from the copper paint, a thin uniform deposit of copper remained on the entire substrate. This deposit was allowed to dry in air, and the cell was subsequently heat-treated and contacted as described above.

A number of experiments were performed in an attempt to determine the optimum conditions of temperature and time for the copper-dip process of barrier formation. These optimum conditions were to be determined by fabricating cells under different temperature and time conditions in an effort to correlate these factors with maximum conversion efficiency. It appears, however, that other variables such as CdS film thickness and certain uncontrollable factors present during vacuum evaporation have an effect on efficiency. Several CdS films deposited at the same time will usually exhibit about the same efficiency when fabricated into photovoltaic cells, provided the barrier forming conditions are identical. However, cells fabricated from two or more separate vacuum evaporations will give variable efficiencies. No definite correlation could be obtained from this series of experiments because of these apparent variations in CdS films from different evaporations and because of the limited

number of cells tested. Temperatures from 59°to 72° C, and processing times from 10 to 60 minutes were used in these experiments. Twelve cells were fabricated with conversion efficiencies between 2.8 and 3.6 percent. In this series of experiments the highest cell efficiency, 3.6 percent, was obtained from a CdS film, 24 microns in thickness, which had been processed in the copper paint at 72°C for 40 minutes.

The nature of the darkened surface or barrier on a CdS film is not fully understood; however, available information indicates that the barrier on a CdS evaporated film is probably some type of surface barrier rather than a barrier produced by the finite diffusion of cuprous ions into the CdS. This conclusion has also been reached by Shirland[1] for the single-crystal CdS photovoltaic cell. In order to investigate further the nature of the barrier surface an evaporated layer was fabricated to permit Hall Mobility measurements. A CdS film was vacuum deposited onto a Pyrex substrate held at 150°C. The thickness of the film was 10 microns, as determined by light transmission interference. This film was treated in such a manner as to produce the darkened surface obtained during photovoltaic cell fabrication. Silver electrodes were then vacuum evaporated onto the darkened surface to permit the Hall Mobility measurement. The result of this measurement indicated that the darkened surface was a p-type semiconductor, with a carrier mobility of 2.5 cm^2/volt-sec. The actual thickness of the dark layer was not known; however, assuming a thickness of one micron, which is probably greater than the actual thickness, the resistivity of the dark layer would be 0.2 ohm-cm and the carrier density would be 10^{19} cm^{-3}. These results are not entirely conclusive, since the dark surface layer was shunted by the underlying layer of n-type CdS and, as indicated, the thickness of the dark surface layer was not known.

The darkened surface on a CdS film can be removed quickly and completely by washing the surface with a dilute acueous solution of KCN. Photovoltaic activity is completely absent after such a treatment. This indicates that any copper which may be present cannot be diffused into the CdS film any great distance.

A portion of a CdS film was converted to single-crystal material by means of the Van Cakenberghe process (Section II). Approximately two-thirds of the film had been converted; the other one-third was left unconverted. When this CdS film, containing both converted and unconverted material, was processed to form a barrier surface by dipping it into 60 ° C copper paint for 30 minutes, only that surface which was not converted (polycrystalline) turned dark. The converted region appeared to have remained unchanged. Careful examination of the film revealed a very slight darkening of the converted region. It appears, therefore, that the rate of darkening was appreciably lessened on the converted region. The conversion process increases the size of the individual crystallites and changes their orientation with respect to the substrate. One or both of these changes might decrease the reactivity of the surface of the

CdS film and consequently change the kinetics of the darkening or barrier formation process. Since the copper paint is held at a temperature of about 60°to 70°C during the barrier formation process, little or no diffusion of cuprous ions into the CdS is expected. A final heat treatment is given to the CdS cells by heating them from room temperature up to 300°C during a 4-minute period. This type of treatment is also expected to cause no cuprous diffusion.

The evidence is certainly not conclusive, but it appears that the nature of the barrier on the evaporated polycrystalline CdS cell may be of a surface-barrier type, formed by the reaction of a reactive CdS surface with copper to form a very thin region of a p-type material, perhaps Cu_2S or Cu_2O.

2. CELL FABRICATION

Certain changes have been incorporated into the thin-film photovoltaic-cell fabrication procedure since the writing of the last Summary Technical Report.

The starting material for the vacuum evaporation was chloride-doped CdS powder. This material is sintered during preparation and is therefore quite dense. In order to free the powder from volatile impurities, it was heated at a temperature of 900°C and at a pressure of 10^{-5} mm Hg for 15 minutes before being used for the CdS evaporation.

It has been found that a substrate temperature of 180°C is more advantageous with respect to adhesion of the CdS film to the substrate during the barrier formation process than a temperature of 150°C. CdS films deposited at 150°C would often separate from the substrate at various small areas during the 300°C heat treatment. When deposited at a substrate temperature of 180°C, CdS films having thicknesses of 24 microns remain adherent to the substrate during subsequent processing. Cells have been fabricated with film thicknesses between 10 and 24 microns, with no observable trend in conversion efficiencies; however, the thinner films have a tendency to separate from the substrate when placed in the etching solution described below. Thicknesses of about 20 to 24 microns can be obtained with evaporation times of about 20 minutes.

A 5-second etch of the CdS film in a 1:1 HCl solution is now employed to provide a clean surface for barrier formation. The film is then rinsed repeatedly in distilled water and finally dried under a heat lamp. The etching process appears to increase the rate at which the CdS film surface becomes dark during barrier formation.

The copper-paint dip process for producing the barrier region, described in detail above, is a modification since the writing of the preceding Summary Technical Report. The final heat treatment of the cell is accomplished by

placing it in a hot furnace and heating from room temperature up to 300°C in an argon atmosphere during a 4-minute period. The cell is then allowed to cool rapidly in the argon. The presence of the copper paint increases the series resistance of the cell. It has been found advantageous to remove the layer of copper paint from the CdS film by means of a suitable solvent after the 300°C heat treatment. Final contact to the darkened surface or p-region of the CdS film can be made with either an air drying silver paint or evaporated silver. The silver paint is very convenient for this step and therefore is generally employed. The final step in cell fabrication is scraping the edge of the CdS film as described previously.

3. TESTING OF CELLS

a. Light Source. The data for all conversion efficiencies reported herein were taken under a tungsten light source. At first, a single 75-watt photospot lamp was used which was powered with 130 volts. The lamp-to-cell distance had been adjusted to produce the same short-circuit current in a CdS film cell as that produced by sunlight, the intensity of which was determined with an Eppley pyrheliometer to be 92 mw/cm^2. A CdS film cell which had been fabricated by means of the older barrier-formation technique described in the first Summary Technical Report was used for this adjustment. The cells formed using the older technique appear to have a different spectral response from cells produced by means of the more recent barrier-formation technique, particularly at longer wavelengths. A subsequent calibration of the light source, made with a freshly prepared CdS cell that was fabricated by the new barrier-formation technique, indicated that the radiation intensity of the light source was about 15 percent greater than the assumed value of 92 mw/cm^2. Such changes in efficiency point up the possibility of errors in arriving at an efficiency value for a specific cell. Obviously, no comparison in efficiencies should be made between cells without first obtaining a clear understanding of the testing method used for obtaining the efficiencies.

When the radiation intensity error was discovered, it was decided to set up a more versatile photovoltaic-cell indoor test arrangement. The previous test arrangement used only one lamp and hence the area of constant illumination was small, being about 4 cm^2. Also, the test arrangement provided no means for filtering out the infra-red radiation which was not usefully absorbed by the cell and served only to increase the cell temperature. Therefore, an illumination source was constructed which consisted of four 150-watt projector flood lamps, arranged at the corners of a square. A one-inch water filter was also installed which served to absorb the infra-red radiation above about 1.1 microns. With this arrangement, a square area of about 20 cm^2 could be uniformly illuminated. The lamp-to-cell distance of this arrangement was adjusted in the manner described above to simulate 100 mw/cm^2 of sunlight radiation. A number of cells, listed in Table I, were measured under this radiation intensity.

TABLE I

SUMMARY OF TEST PARAMETERS FOR
31 CdS THIN-FILM CELLS

Cell No.	Thickness (microns)	Area (cm^2)	Light Intensity Tungsten Lamp (mw/cm^2)	Open Circuit Voltage (v)	Short Circuit Current (ma)	Efficiency (%)
R-77-2A	18	0.68	92	0.50	11.0	3.50
R-77-2B	18	0.50	92	0.48	8.5	3.74
R-87-1	17	1.47	92	0.475	24.5	3.30
R-87-2	17	1.70	92	0.44	20.0	1.89
R-87-3	17	1.70	92	0.48	21.5	2.41
R-87-4	17	1.61	92	0.52	18.5	2.31
R-90-1	6.2	1.50	92	0.38	17.2	2.12
R-91-2	10	1.70	92	0.445	22.0	2.93
R-96-1	14	2.38	92	0.40	44.0	2.93
R-97-1	19	7.7	92	0.46	100	1.91
R-97-2	19	5.9	92	0.46	76.0	2.28
R-98-1	23	1.53	92	0.48	30.0	3.99
R-98-2	23	1.62	92	0.48	36.0	4.48
R-99-3	22	1.52	92	0.425	22.0	3.25
R-99-4	22	1.34	92	0.46	16.5	3.38
R-100-1	16	1.54	92	0.46	26.0	4.21
R-100-2	16	1.60	92	0.48	16.5	2.75
R-100-3	16	1.61	92	0.52	16.5	2.50
R-100-4	16	1.05	100	0.51	9.4	3.04
R-101-1	24	1.69	100	0.45	19.5	3.04
R-101-2	24	1.54	100	0.48	19.0	2.96
R-101-3	24	1.55	100	0.47	17.0	3.07
R-101-4	24	1.64	100	0.465	18.5	3.34
R-102-1	15	4.37	100	0.44	49.5	2.44
R-103-1	24	1.62	100	0.47	20.0	3.61
R-103-2	24	1.66	100	0.48	19.5	3.10
R-103-3	24	1.52	100	0.46	20.0	3.50
R-103-4	24	1.57	100	0.44	21.5	3.34
R-104-2	16	1.61	100	0.495	15.8	3.03
R-104-3	16	1.65	100	0.50	15.5	3.02
R-104-4	16	1.53	100	0.51	13.0	2.80

b. Current-Voltage Characteristic and Efficiency. The efficiencies of the CdS thin-film cells were determined by varying the load resistance of the cells and measuring the voltage and current while the cells were illuminated. The maximum power a cell can deliver, P_{max}, is represented by the area of the largest rectangle that can be fitted under the curve. Figure 1 shows the current-voltage curve for cell R-103-1. This cell was fabricated by means of the copper-paint dip process; the rectangular shape of the curve is to be noted. At 100 mw/cm^2, an open-circuit voltage of 0.47 volt and a short-circuit current of 12.3 ma/cm^2 was obtained. The maximum power this cell could deliver was 3.61 mw/cm^2; the efficiency was 3.61 percent. For this cell the maximum deliverable power was 62 percent of the product to the open-circuit voltage and short-circuit current density. Good single-crystal cells produce maximum power of about 60 to 75 percent of the product of the open-circuit voltage and the short-circuit current.

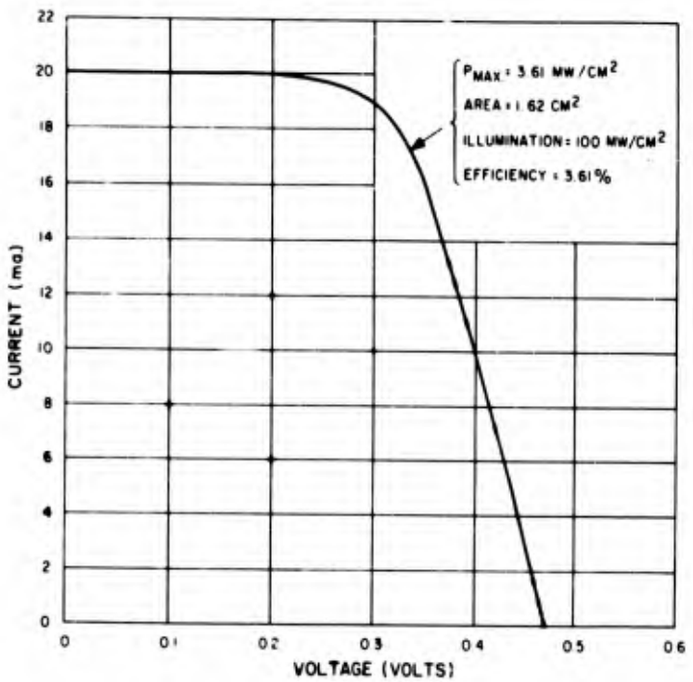

Figure 1. Current-Voltage Characteristic of CdS Thin-Film Photovoltaic Cell

Table I contains a listing of the film thickness, cell area, intensity of test lamp, open-circuit voltage, short-circuit current, and efficiency for a number of CdS thin-film cells.

c. Spectral Response. The spectral response of cell R-91-2 shown in Figure 2 was determined with a Bausch and Lomb grating monochrometer containing a tungsten light source. The cell response was normalized to take into consideration differences in the spectral intensity transmitted by the monochrometer. This cell had an active area of 1.7 cm^2 and exhibited an efficiency of 2.93 percent. The spectral response of this cell is different from that of less efficient cells fabricated by means of the older barrier-formation technique. The dashed line in Figure 2 is the spectral response of cell R-34 as reported in the previous Summary Technical Report. Two differences may be noted. First, the peak of the curve at wavelengths slightly greater than the absorption edge (0.52 micron) is much broader in the more efficient cell. Second, the broad peak at about 0.85 micron for cell R-34 is completely absent for cell R-91-2. These differences can probably be attributed to the different barrier formation procedures used to fabricate the two cells. An observed change in the spectral response of CdS single-crystal cells of different efficiencies has been pointed out by Shirland [1]. In this case the spectral response becomes

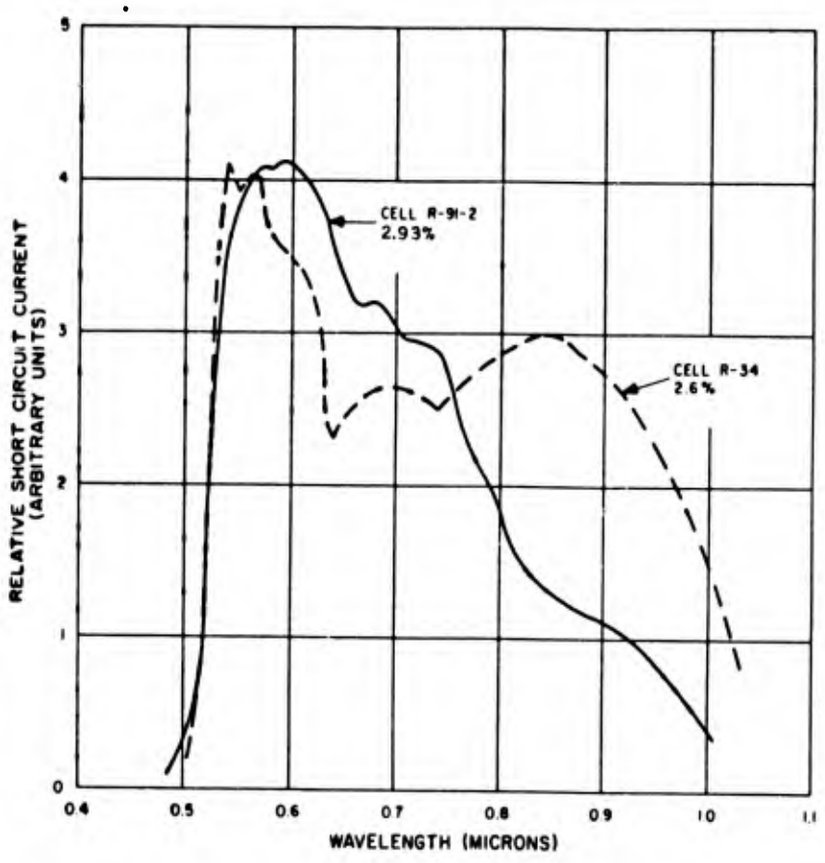

Figure 2. Spectral Response of CdS Thin-Film Photovoltaic Cells

narrower as the conversion efficiency of the cell improves. This change in spectral response was explained by Shirland to be the result of holes formed in the n-type region near the barrier that have diffusion lengths comparable to the barrier thickness. Thus a higher proportion of the holes generated in the n-region contribute to the cell output and result in a higher efficiency over a narrower spectral range. Even though more holes are formed by longer wavelength photons, they are generated at distances too far from the barrier to be effective.

4. CELL DETERIORATION

It has been observed that CdS thin-film photovoltaic cells are unstable, and that unless they are protected from the atmosphere after fabrication they deteriorate, as indicated by the decrease of short-circuit current and efficiency. At one time it was thought that the efficiency of an unprotected cell would decrease steadily for a period of about one month and then level off. Recent measurements, however, indicate that the cell continues to degrade with time. The decrease of efficiency does not appear to be linear with time. Instead, efficiency drops sharply for a few days after fabrication and decreases at a much slower rate thereafter.

The nature of cell degradation is perplexing and differs from cell to cell. One or two days after cell fabrication, the short-circuit current may drop by 5 percent, the open-circuit voltage may increase by 2 to 4 percent, and the current-voltage characteristic may become slightly more rectangular. In these cases the efficiency may be the same as that measured immediately after fabrication. This condition does not last very long. Cell efficiency soon starts to drop, and the open-circuit voltage returns to its initial value. The rate of deterioration appears to be different for different cells and may be a sensitive function of the ambient humidity.

Previous tests indicated that deterioration can be retarded if the cell is stored in a dry inert atmosphere, or if it is protected by means of a thin plastic film applied as a spray paint. Three methods for protecting the CdS cells have been tried. These methods include coating the cell surface with a thin layer of epoxy resin, storing the cell in a desiccator, and storing the cell in a vacuum. Another method which has been tried involves coating the exposed surface of the cell with a few microns of a polystyrene layer, using a glow-discharge process. This method is discussed in Section III of this report.

If epoxy resin is used as a protective cover, it must be cured at a reduced pressure (0.1 mm Hg) and at an elevated temperature (50°C) to prevent moisture pickup during the cure period. Vacuum storage of the cells was conducted at a pressure of 10^{-5} mm Hg. Cells which were stored in a desiccator were first placed in a closed lucite box. The lucite box was then placed in a desiccator containing $CaSO_4$ as the desiccant. Figure 3, which relates percentage decrease of efficiency to time, shows the results of the above tests. Unfortunately, sufficient data were not taken for two of the cells to permit interconnection of the points by means of a curve. One cell was left in room air without any protection. This unprotected cell had an initial efficiency of 3.34 percent. At the end of a 46-day period the efficiency of this cell had dropped to 0.25 percent. The cell that was protected by a thin layer of epoxy

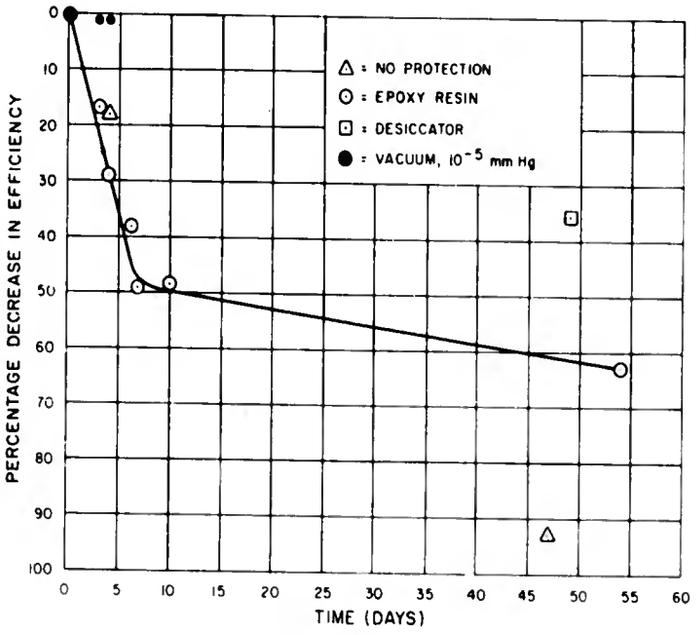

Figure 3. Efficiency Decrease Vs Time for CdS Thin-Film Photovoltaic Cells Protected by Various Methods

resin had an initial efficiency of 2.75 percent after the resin had cured. The efficiency of the resin-protected cell dropped to 1.4 percent during the first 7 days and to 1.03 percent during the next 47 days. The cell that was placed in the desiccator had an initial efficiency of 3.1 percent. At the end of 49 days the efficiency of this cell had decreased to 2.0 percent. The vacuum protected cell was in a vacuum for a period of only 4 days. However, at the end of this period cell efficiency had dropped from 3.50 percent to 3.46 percent, a drop of only 0.04 percent.

The results described above indicate that the efficiency deterioration of the CdS thin-film cells being fabricated at present can be retarded by protecting the barrier from the atmosphere. The best protection is a vacuum condition; however, an extremely dry ambient is also beneficial. Encapsulation of the barrier with a suitable resin also shows considerable promise provided that the resin is impermeable to moisture and does not give off any deleterious substances during cure or afterwards.

5. LARGE AREA CELLS

A number of attempts have been made to fabricate polycrystalline CdS thin-film cells with active areas between 10 and 20 cm^2. These attempts have not been very successful. One major problem is the relatively high series resistance presented by the transparent tin-oxide electrode. This problem is not serious for cell areas of 2 to 4 cm^2. When the cell area is greater than 5 cm^2, however, a high series resistance is a major factor limiting efficiency.

Two approaches to the problem of reducing resistance of the transparent electrode have been tried. Evaporation of a thin gold film onto a tin-oxide coated substrate was tried. This approach met with little success. The resistance of the tin oxide was not changed noticeably until the gold was thick enough to reduce the optical transmission by 50 to 60 percent. In addition, the gold deposit was easily scratched. The second approach involved the vacuum evaporation of silver stripes onto a tin-oxide coated substrate. These stripes were 6 mm apart, approximately 0.4 mm wide, and about one micron thick. The stripes did not serve the intended purpose because the evaporated CdS films did not adhere to the silver during the subsequent barrier forming process. We intend to try this technique with other metals such as zinc and gold.

The total amount of time spent on the large-cell-area problem is quite small. Most of the effort has been expended on small, easily handled cells in order to determine optimum conditions for cell fabrication.

6. RADIATION DAMAGE

A light-weight photovoltaic cell of the polycrystalline CdS thin-film type would be, in most respects, ideally suited for satellite power supplies. A major factor which must be evaluated, however, is the damage experienced by such cells when bombarded by the high-energy particles associated with the Van Allen radiation belts. An exploratory test was performed to determine the damage experienced by a CdS thin-film cell subjected to bombardment by 0.8 Mev electrons. Electron irradiation was produced by means of a 1-Mev Van de Graaff generator.

Since Pyrex would have been discolored by radiation, a piece of 1/16-inch quartz coated with tin oxide was selected as the substrate for the test cell. The cell was bombarded on its front face; had the substrate side been exposed to bombardment, the quartz would have absorbed much of the electron energy. To prevent absorption by the silver paint contact to the front face of the cell, the contact was modified to the form of an annular ring which covered only a portion of the surface. The cell was tested as a frontwall cell before bombardment by illumination with the tungsten light source. The cell was then bombarded with a total flux of 9.7×10^{15} electrons/cm^2. The quartz substrate, probably of a poor quality, experienced considerable radiation discoloration, becoming quite brown. After bombardment, the cell was again tested as a frontwall cell, using the same illumination. The shape of the current-voltage curve was quite poor because the silver-paint electrode only contacted a small area of the p-region and the sheet resistance of the p-region was quite high. The short-circuit current, open-circuit voltage, and efficiency of the cell had decreased by 10.2, 4.3, and 11.1 percent, respectively, as the result of bombardment. Part of this decrease may have been due to the radiation discoloration experienced by the substrate. Even though the cell was tested as a frontwall cell, the darkening of the substrate could reduce the amount of light reaching the barrier by reflection through the substrate. The radiation damage study will be conducted again using as the cell substrate a piece of polished sapphire, which is resistant to radiation discoloration.

The electron bombardment results may be compared with results obtained at the RCA Laboratories. Silicon n-on-p photovoltaic cells were subjected to the same electron energy and approximately the same total flux as in the test described above. The short-circuit current and efficiency decreased by about 32 percent and 40 percent, respectively. It should be borne in mind, however, that the Si and CdS cells compared here did not have the same initial efficiency. The initial efficiency of the Si cell was 5.4 percent while that of the CdS cell was only 0.72 percent because of the modified electrode and frontwall operation of the cell. It is not possible to say whether a 5-percent CdS cell would degrade to the same extent as the 0.72-percent cell.

7. THIN SUBSTRATES

In order to achieve the advantage in watts per pound that the thin-film photovoltaic cell promises, it will be necessary to fabricate these cells on light-weight substrates. To this end an attempt was made to fabricate a cell on a piece of 0.004-inch glass which had a tin-oxide layer with a resistance of about 30 ohms/square. A CdS film 16 microns in thickness was vacuum evaporated onto this substrate. This film was fabricated into a photovoltaic cell by the procedure described previously. Great care had to be exercised

in the fabrication of this cell because of the fragility of the substrate. The cell had an active area of 1.5 cm^2, an open-circuit voltage of 0.47 volt, a short-circuit current of 13 ma, and an efficiency of 2.28 percent as determined under a tungsten light source calibrated to simulate 100 mw/cm^2 of solar radiation. Figure 4 shows a photograph of this cell. The photograph also shows a cell deposited on 0.062-inch glass. These pictures were taken with a mirror situated behind the cells in order to show both the front and the back surfaces.

SUMMARY AND CONCLUSIONS WITH RESPECT TO PHOTOVOLTAIC MATERIALS

The best CdS thin-film photovoltaic cell produced to date exhibits an efficiency of about 4.5 percent and has an active area of 1.62 cm^2. Most of the fabricated cells have efficiencies between 3 and 3.5 percent and active areas of about 1.6 cm^2. The present fabrication procedure uses CdS films about 20 microns thick which are formed by vacuum evaporation of CdS powder onto transparent conducting substrates heated to 180°C. The surface of the film is etched in 1:1 HCl and the barrier is formed on the surface of the film by placing the cell in a 70°C copper-paint bath for about 40 minutes. The bath consists of finely divided copper in a lacquer vehicle. A final heat treatment in an inert atmosphere is given to the cell by heating to 300°C during a 4-minute period. The dried copper paint on the surface of the CdS film is removed and electrical contact to the barrier surface is made with either silver paint or vacuum evaporated silver.

Recent work has placed considerable emphasis on improving the barrier-formation procedure. The complexity of cell fabrication has been reduced and reproducibility has been improved. The nature of the darkened surface that forms on the surface of CdS films during barrier formation is believed to be some type of surface barrier rather than a barrier produced by the diffusion of cuprous ions into the CdS.

The deterioration of cell efficiency with time seems to be caused by moisture in the air. Protection of a cell by encapsulation or storage in a dry ambient can significantly retard the rate of deterioration. Enclosure of the cell in a vacuum appears to be the best protective measure.

The fabrication of large-area cells, 5 cm^2 and greater, at present appears to be limited by the high series resistance presented by the transparent electrode. Initial attempts at solving this problem by the use of evaporated metallic stripes have not been successful.

The radiation damage characteristic of a CdS thin-film cell subjected to 0.8-Mev electrons was determined. The results of this test indicate that polycrystalline CdS thin-film cells withstand bombardment as well as, and probably better than, n-on-p silicon cells, with respect to the percentage decrease in efficiency.

A relatively successful attempt was made at fabricating an evaporated CdS cell on a 0.004-inch glass substrate. This cell had an efficiency of 2.28 percent. The use of thin substrates is mandatory if advantage is to be taken of the high watts per pound that the thin-film technique promises.

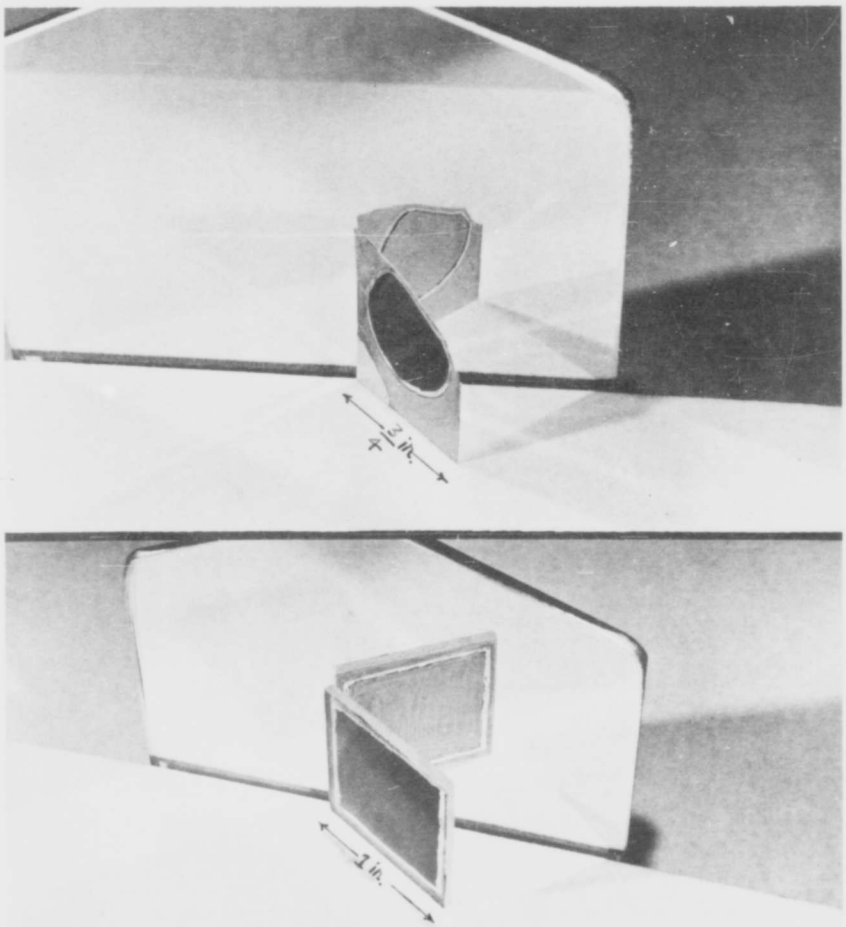

Figure 4. CdS Thin-Film Photovoltaic Cells on Two Types of Substrates

II. CRYSTAL LAYER CONVERSION

INTRODUCTION

Photovoltaic cells made from bulk single crystals of cadmium sulfide have efficiencies of 6 to 8 percent. As described in Section I of this report, cells made from vacuum deposited microcrystalline films have not shown efficiencies greater than 5 percent. A method now exists for recrystallizing these microcrystalline films to form single crystals with lateral dimensions of several millimeters. From such films it should be possible to produce cells having efficiencies comparable to those of cells made from bulk single crystals without sacrificing the advantages inherent in the use of large area thin-film material.

The objectives of the study described in this section have been:

a. To determine the mechanism by which recrystallization takes place, in order that good control of the process can be achieved, and in order that the laws governing the process can be learned and applied to other materials, and

b. To evaluate the electrical properties of recrystallized films and the photovoltaic response of cells made from recrystallized films.

In the preceding Summary Technical Report the procedure for recrystallizing films was described in some detail, and it was pointed out which steps in the procedure are critical and which are not. Detailed descriptions of the recrystallization process and of the film structure before and after recrystallization were also given. Preliminary results of measurements of film resistivity and Hall mobility were reported.

In the work covered by this report two main methods of attack have been emphasized:

a. Macroscopic observations of the recrystallization process have continued. For these observations, certain parameters, including substrate material, activator material, ambient gases, and temperature during recrystallization have been varied. Observations were made of speed of crystal growth, general texture of the recrystallized films, and temperature of nucleation.

b. Optical and electrical measurements have been made on the films both before and after recrystallization in an effort to determine what changes occur in the energy states of the crystals, i.e., what states may be introduced by the activator (silver or copper), what other impurity states are present and how these various states may interact. Such measurements include optical absorption as a function of wavelength, photosensitivity, spectral sensitivity of photoconductivity and thermally stimulated current. It is expected that more emphasis will be placed on Hall effect measurements in the future.

TECHNICAL DISCUSSION

1. EFFECT OF OXYGEN ON RECRYSTALLIZATION

Normally only an inert gas (argon) is present in the oven during the recrystallization process, and films normally recrystallize at some temperature between 470° and 570° C. If, however, a small amount of oxygen is bled into the oven at about one tenth of the argon flow rate, recrystallization will occur at much lower temperature, in some cases as low as 300° C. Crystal growth is much slower at the lower temperatures and may not even be constant, especially at the lowest temperatures. Growth tends to be slower in a direction perpendicular to the edge of the film when it is close to an edge. The growth front tends to be very ragged, and some parts of the front may grow faster than others. Also the film nucleates at many points rather than at one or only a few points. The resulting film has a rather poor appearance as shown in Figure 5, with many relatively small crystals of very irregular shapes. Their structure, however, appears to be basically the same as that of the larger crystals, usually obtained at the higher temperatures. They contain many small angle grain boundaries which give them the same feathery appearance which is characteristic of the larger crystals.

2. SPEED OF GROWTH

When it was first discovered that oxygen would cause recrystallization to occur at lower temperatures, a study of the kinetics of recrystallization by measuring the speed of growth as a function of temperature was planned. The temperature could be set at some desired value below that at which recrystallization would occur without oxygen. Oxygen could then be admitted to cause recrystallization to occur at that temperature.

The results of measurements of growth speed are shown in Figure 6, which is a plot of log growth speed relative to reciprocal temperature. The large scatter in the data is immediately evident. At the lower temperatures,

Figure 5. Film Recrystallized in a Partial Oxygen Atmosphere (67X); Crossed Polaroids

scatter may appear in the data from one film, as discussed above. For example, the three points at 1000/T = 1.55 were measured on the same film; this is also true of the two points at 1000/T = 1.48. At the higher temperatures, with no oxygen present, no scatter was observed in the data from any one film, but it is clear from Figure 6 that a considerable scatter exists in the data from different films.

Also evident in Figure 6 is the general trend toward slower growth at lower temperatures. Simple rate theory predicts that the growth speed (G) is given by:[4]

$$G = G_o \exp(-Q/kT)$$

where Q is the activation energy for the process, k is Boltzmann's constant, T is the absolute temperature, and G_o is a constant (independent of temperature) which depends on such quantities as the entropy of activation and the free energy difference between the recrystallized and uncrystallized states. If this theory were valid, the data shown in Figure 6 would fall on a straight line. To account for deviations from a straight line, the theory can be modified by allowing G_o to vary with temperature. This may be justified, for example, if inclusions are present in the material and their number or size varies with temperature. The present case must be somewhat more involved, since growth

speed is not only a function of temperature but varies with different films and even with different parts of the same film. It might be possible, however, to

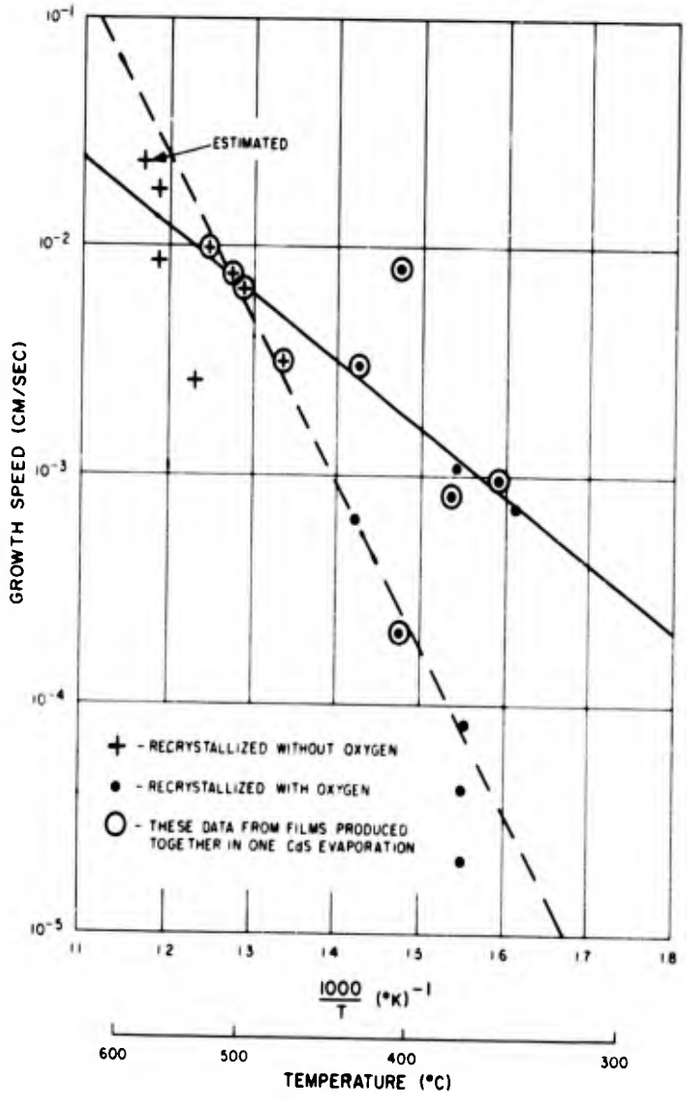

Figure 6. Log Growth Speed Vs Reciprocal Temperature

account for the observed variations by an inclusion hypothesis. The variations in G for different films might reflect different amounts or types of inclusions incorporated in the films during the CdS evaporation process. The variations in G for different parts of the same film might be due to a non-uniform distribution of inclusions in the film. The apparent existence of a critical temperature below which recrystallization does not occur may indicate that the solution temperature of the inclusions must be reached before recrystallization can occur. The interaction of oxygen with the inclusions may form a phase with a lower solution temperature.

This hypothesis has very little foundation at present. The role of the silver in this model has not been postulated. However, it is known that imperfections in these films can inhibit crystal growth. In one film, for example, circular areas of about 10-microns radius surrounding three relatively large imperfections did not recrystallize, and it has been observed that large cleavage steps in mica substrates are effective barriers to crystal growth. Also there seems to be some unknown parameter associated with the CdS evaporation process which determines some of the subsequent recrystallization properties of the films*. Most notable of these is the critical temperature. The unknown parameter is very likely the number or types of impurities (or inclusions) which enter the films during their formation. In order to test some of these ideas, more emphasis will be placed on attempts to control or limit the impurities which are incorporated in the films during their formation.

In order to give an indication of the range of possible values for G_o and Q, the values have been computed for the two straight lines drawn in Figure 6. The values are:

Solid Line	Dashed Line
G_o = 50 cm/sec	$G_o = 7 \times 10^6$ cm/sec
Q = 14 kcal/mole	Q = 32 kcal/mole

3. EFFECT OF OTHER ACTIVATORS ON RECRYSTALLIZATION

Van Cakenberghe [2,3] has claimed that although silver is the most successful activator for promoting the recrystallization of CdS, other activators could be used. Three activators other than silver have been tested in connection with the present work; these are copper, indium, and lead. So far no sign of

*The behavior of all samples produced together in a single CdS evaporation tends to be similar, but the behavior of samples produced by different CdS evaporations [4] may be quite different.

recrystallization has been obtained with either indium or lead.* However, films have been successfully recrystallized using copper as the activator. Recrystallization with copper differs from that with silver in two main respects. The recrystallization temperature is considerably lower (350 to 400° C with copper compared to 475 to 575° C with silver), and the CdS crystals in the recrystallized films are considerably smaller. The effect on crystal size of using a copper activator can be seen clearly in Figure 7. For this film the CdS was deposited in several strips. The strips in the upper half of the picture were recrystallized with copper and contain many relatively small crystals; those in the lower half were recrystallized with silver and contain much larger crystals with the typical feathery appearance indicative of small angle grain boundaries.

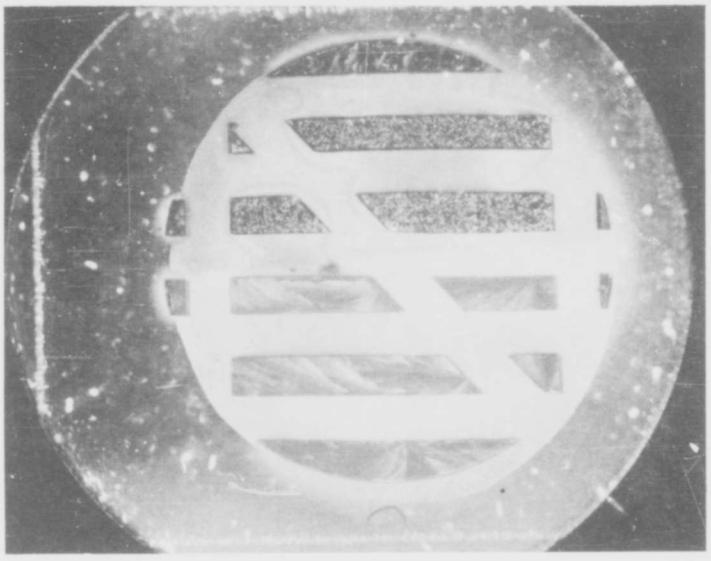

Figure 7. Effects of Different Activators: Cu (top strips) and Ag (bottom strips) (4.5X); Crossed Polaroids

4. EFFECT OF RECRYSTALLIZATION ON OPTICAL ABSORPTION

Room temperature optical absorption measurements at wavelengths between 5000 and 8500 A have been made on several films, both before and after recrystallization. Typical results are shown in Figure 8. The effect of recrystallization is to shift the apparent fundamental absorption edge (from about 5200 A) to slightly shorter wavelengths and to increase the absorption for wavelengths greater than about 5500 A. An absorption peak at about 6000 A is almost re-

* Other workers have claimed partial success with indium on CdS films that had been especially treated in sulfur vapor.[5]

solved. Absorption due to acceptor states formed by silver in the lattice (usually assumed to be in substitutional sites) is normally found at about this position; therefore it appears that some of the silver has entered the CdS lattice to form such states. The shift in the apparent absorption edge may be due to the elimination of some of the excess cadmium normally present in evaporated CdS films. This shift corresponds to the observed change in color of the films from orange-yellow to yellow.

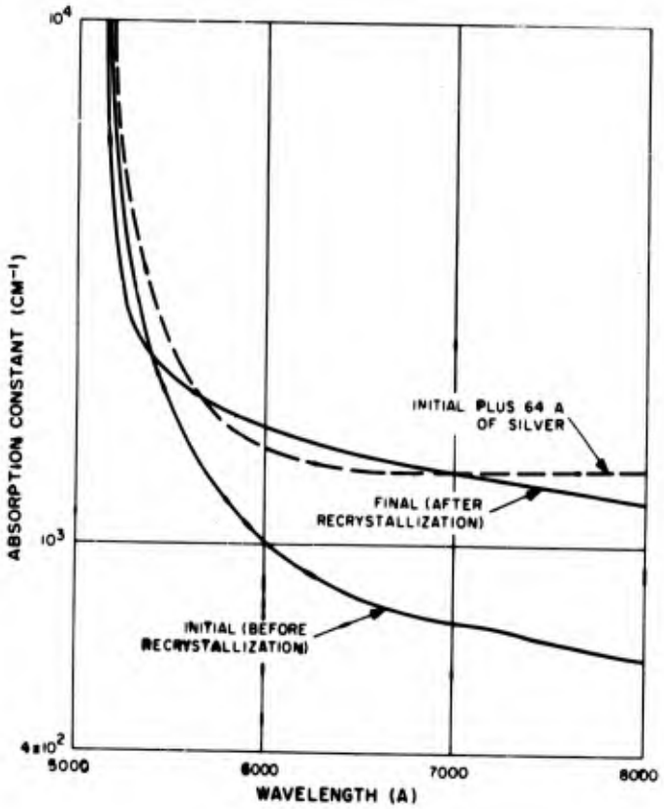

Figure 8. Optical Absorption by CdS Films at Room Temperature

5. EFFECT OF RECRYSTALLIZATION ON PHOTOCONDUCTIVITY

Measurements of the spectral response of the photocurrent in recrystallized films tend to confirm the presence of the typical acceptor states formed by silver in the CdS lattice. The presence of these states was first suggested by optical absorption spectra, as discussed above. A typical response is shown in Figure 9. The curve has a maximum at about 5100 A, resulting from transitions across the band gap. Some contribution at longer wavelengths, due to the silver acceptors, is apparent. From the relative intensities of these contributions, it is estimated that the concentration of acceptor states formed by the silver is not more than about ten parts per million. Copper can also form similar acceptor states in CdS. Figure 10 shows a spectral response curve obtained from a film recrystallized with copper. This curve is

similar to Figure 9 except that the contribution at longer wavelengths, due to the copper acceptors, is more clearly defined.

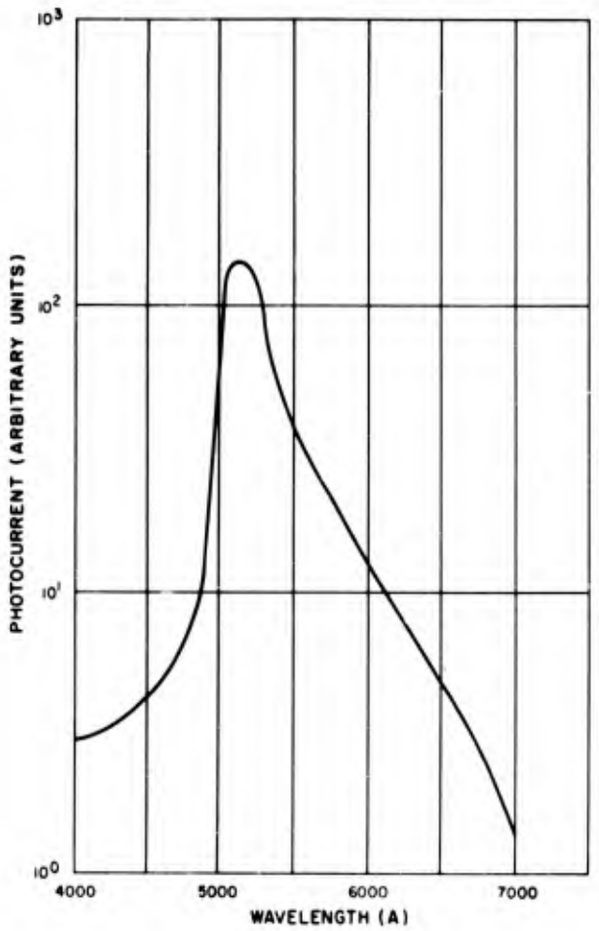

Figure 9. Spectral Response of Photoconductivity; Recrystallized Film; Silver Activator

The photosensitivity* of the recrystallized films is nearly always several orders of magnitude greater than that of the unrecrystallized films, although it varies considerably among different recrystallized films. Almost the entire increase in sensitivity can be attributed to a decrease in the dark conductivity. Dark conductivities of recrystallized films are usually in the range of 10^{-8} to 10^{-9}/ohm cm; for unrecrystallized films which have been heat treated the values are in the range of 10^{-4} to 10^{-5}/ohm cm. However at reasonable light levels of 10 ft-c or greater the photoconductivities of recrystallized and unrecrystallized films are comparable in most cases, and in a few cases the photoconductivity of the recrystallized films exceeds that of the unrecrystallized films

* Photosensitivity is defined as the ratio of photoconductivity (the conductivity (σ) with light incident on the sample) to the dark conductivity (σ_o). It is therefore a function of incident light.

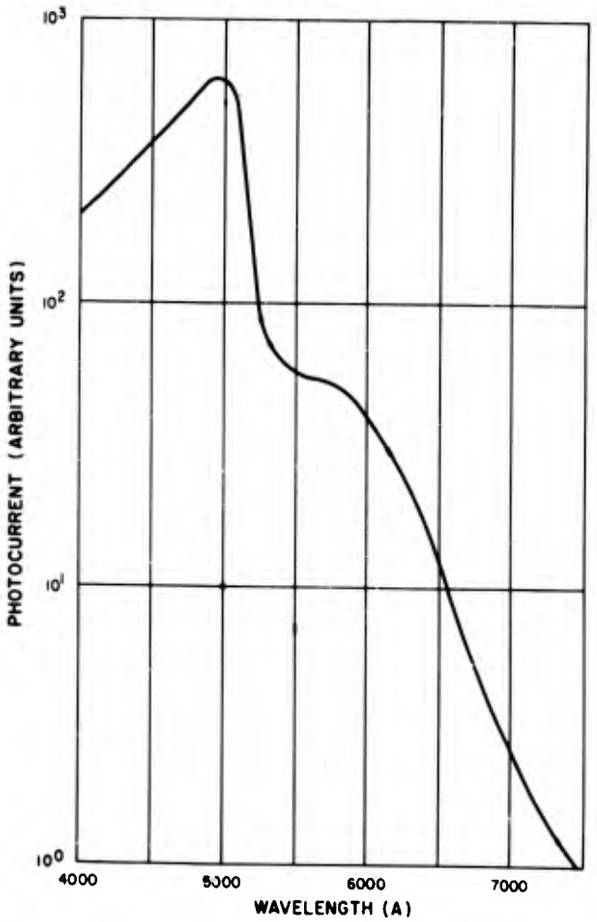

Figure 10. Spectral Response of Photoconductivity; Recrystallized Film; Copper Activator

at very high light levels (1000 ft-c). These facts indicate that the low dark conductivities of recrystallized films may not be detrimental to their application in photovoltaic cells that are normally operated at high light levels.

During the photosensitivity measurements it was observed that rise and decay time constants were quite long (on the order of several minutes), suggesting the presence of a high concentration of traps. This is verified by a measurement of the thermally stimulated current as shown in Figure 11.

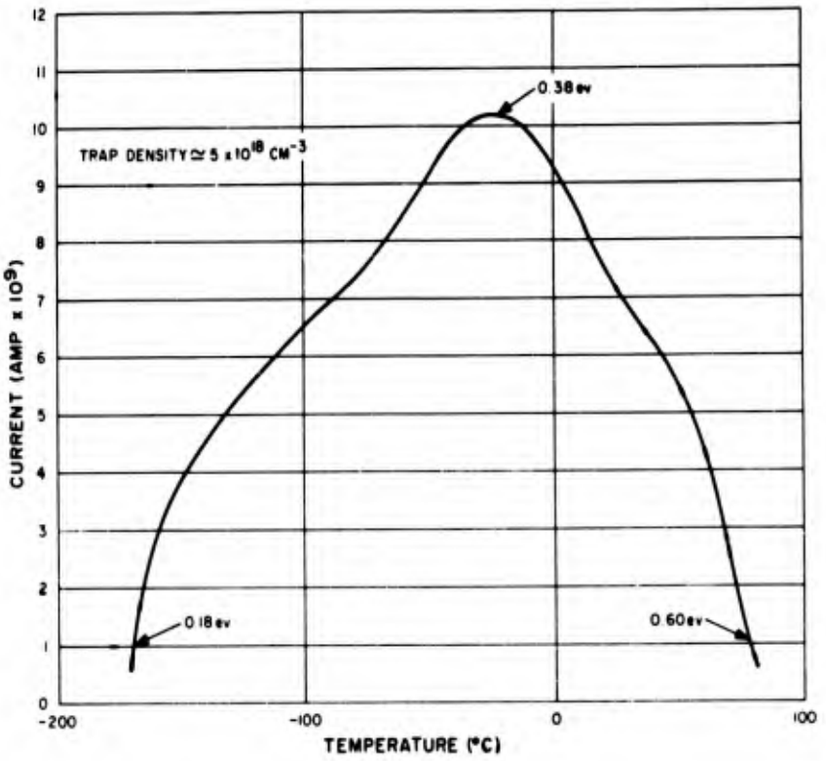

Figure 11. Thermally Stimulated Current

This indicates a very broad distribution of compensated donor centers (traps) from about 0.18 ev to about 0.60 ev; the distribution has a maximum at about 0.38 ev, and contains a total trap concentration of about 5×10^{18} cm^{-3}. In addition, measurements of conductivity versus temperature indicate that not all of the donor centers in this energy range are compensated. Therefore, if donor centers due to excess cadmium have been removed by the recrystallization process, as suggested by the optical absorption data given above, it is clear that a high concentration of donor type impurities must be present. These impurities were probably introduced during the deposition of the CdS, and may play an important role in the recrystallization process.

From these results it is apparent that the increased resistivity of recrystallized films is not due to removal of the donor centers which are present in the unrecrystallized films, but is due to the partial compensation of these states by the acceptor states which are formed during the recrystallization process. Some, or perhaps all, of these acceptor states are provided by the silver or copper activator.

It is interesting to speculate about the role of the activator in the recrystallization process. When the electrons from the donor states fall into the acceptor states formed by the activator, a decrease in the electronic contribution to the energy of the crystal results. This decrease is between one and two electron-volts for each transition. An increase may take place in the lattice free energy

because of the occupation of substitutional sites by the activator atoms, but this increase is probably less than one electron-volt per atom. The net result is a decrease in free energy due to the formation of the acceptor states during recrystallization. This may be the source of the free energy change that is required for the recrystallization process. If so, it would explain why activators such as indium, which form donor states in CdS, do not work unless the initial electronic configuration of the CdS films can be changed. Such a change might be effected by controlling the impurities which enter the films during their formation, or by subsequently processing the films in controlled atmospheres. Another possible role of the activator might be to interact with impurities to form a soluble phase which would lower the free energy for crystal growth.* At present it is uncertain whether either, or perhaps both, of these proposed mechanisms is operating. To obtain a clue, it is important to gain control over the impurities which enter the films during their formation. It is expected that this may be accomplished by modifying the CdS evaporation setup. With the present setup, there is good evidence to indicate that residual gases in the vacuum system interact with the films. A setup which would prevent this interaction might afford the desired control.

6. CONTACT TO THE SUBSTRATE

It had been observed previously that samples recrystallized on Pyrex substrates, or Pyrex substrates coated with a transparent conducting coating of tin oxide, have a tendency to separate from the substrate. At that time this effect had not been observed when substrates of soft glass were used. However more recent experiments with very thick CdS films (15 microns or more) indicate that separation from the substrate after recrystallization can also occur on soft glass substrates. Also there is some indication that electrical contact between the recrystallized film and the substrate may be broken[5] even in those films for which the separation has not occurred to an extent that can be detected visually. From the visual observations it appears that the tendency of the recrystallized films to separate from the substrate is greater for the glass substrates with the lower thermal expansion, and also is greater for the thicker CdS films. These facts are consistent with the hypothesis that the stress induced by the differential thermal expansion between the film and substrate can be relieved in the grain boundaries of the microcrystalline films, but breaks the bonds between the film and the substrate in the recrystallized films which contain large coherent crystals.

---

* Exaggerated growth after the solution of a dispersed phase in aluminum alloys has been observed by Beck, Holzworth, and Sperry.[6]

A solution to this problem may be found in the use of a substrate material having a thermal expansion coefficient closely matching that of the CdS (approximately 6 x 10^{-6} per ° C), [7] or perhaps in flexible substrates which can relieve the stress by flexing. The problem may also be minimized by using the thinnest films compatible with their application. This problem must be solved before any device such as a photovoltaic cell can be fabricated from these films.

In most cases where separation occurs, random cracks appear in the films, and patches which lift off the substrate can be seen. However, in one film an unusual effect was observed. Striations appeared which were all parallel in any one crystal, but ran in different directions in different crystals (Figure 12 is a photograph of this film showing the effect). Most of the striations were continuous across the entire film, changing their direction as they crossed the boundary between crystals. X-ray analysis of various parts of this film, using the Laue back reflection method, indicates that the striations are parallel to the projection of the c-axis on the film surface. This was found to be parallel to the line of intersection between the surface and (110) planes in some crystals and (100) planes in another crystal. It is tempting to postulate that these striations might be slip bands which were formed to relieve stress in the film, but apparently a (110) slip system has not been observed previously in bulk CdS crystals. [8]

Figure 12. Film with Striations (5X); Crossed Polaroids

A Laue back reflection photograph of one of the crystals in the striated film is shown in Figure 13. The fact that each "spot" is actually a collection of several small spots, slightly displaced from each other, tends to verify the interpretation of the feathery substructure seen through crossed polariods; many small angle boundaries are present within a large crystal. Within the area of the x-ray beam (1/2 mm diameter), the total angular variation between these subgrain boundaries is less than two degrees.

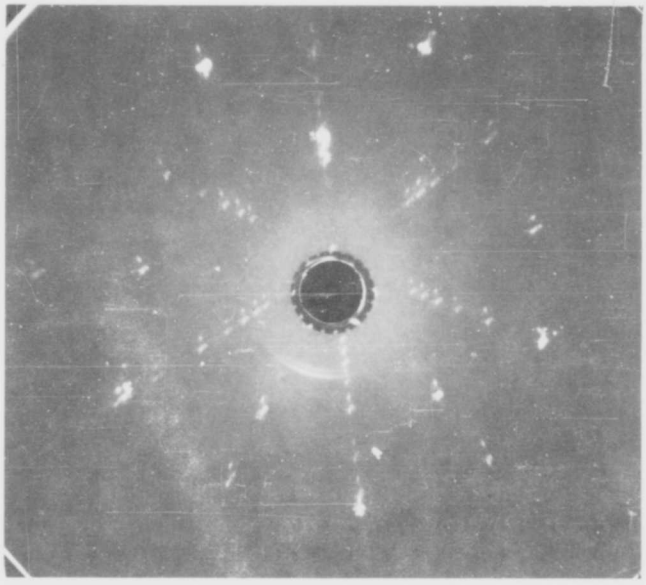

Figure 13. Laue Pattern from a Recrystallized Area

7. INVESTIGATION OF MICA SUBSTRATES

In anticipation of future needs for a very flexible substrate material, an attempt was made to recrystallize a film on a cleaved mica surface. Preliminary x-ray results indicate that the microcrystalline CdS film deposited on mica, itself a crystalline material, is similar to that on glass with regard to orientation and crystal size. The attempt to recrystallize the film using a silver activator was successful, but in some respects the recrystallization was similar to that of films on glass with oxygen present, although no oxygen was admitted to the oven. The recrystallization temperature was unusually low (450 ° C), and the growth speed varied considerably. It was also noted that large cleavage steps in the mica were an effective barrier to motion of the growth front.

SUMMARY AND CONCLUSIONS WITH RESPECT TO CRYSTAL LAYER CONVERSION

Recrystallization was found to occur at lower temperatures (300-350 ° C) when a small amount of oxygen is present in the oven. Under these conditions crystal growth is considerably slower than at higher temperatures, and tends to vary considerably during recrystallization of a given film.

Attempts were made to use activators other than silver for the recrystallization process; copper, indium, and lead were tried. Of these attempts the only successes were with copper. In general, recrystallization occurs at a lower temperature and the crystal size is smaller when copper is used rather than silver.

Photoconductivity measurements indicate that the high resistivities found for the recrystallized films are due to compensation of the donor states normally present in the microcrystalline films, rather than to removal of these donor states. Therefore, a high density of traps is present, and photoconductivity time constants are large. However photosensitivities are quite large, and conductivity under illumination is in some cases higher than that of the heat-treated microcrystalline films. The conductivity may be sufficiently high for applications such as photovoltaic cells, where low resistivity material is needed.

Data taken on recrystallized films indicate that impurities incorporated in the films during their formation determine the subsequent recrystallization properties of the films. The concentration or type of impurity in a film apparently affects the recrystallization temperature and the speed of growth of the film. The type of impurity may determine the type of activator that is required. Therefore, efforts to control or limit the impurities which enter the films during their formation will be important for obtaining a more complete understanding of the recrystallization process.

The problem of making intimate contact between the recrystallized CdS films and the substrates is greater than initially anticipated. It was previously noted that films tend to separate from Pyrex glass but not from soft glass; it is now found that very thick films (15 microns or greater) also separate from soft glass. In addition there is evidence which suggests that the electrical contact to the substrate may be poor even though the film has not mechanically separated from the substrate to an extent that can be observed visually. This condition is probably the result of differential thermal expansion between the substrate and the very coherent single crystals of the recrystallized films. A method for maintaining good electrical contact between the film and the substrate must be found before satisfactory photovoltaic cells can be fabricated from these films.

III. Cds CELL FABRICATION

INTRODUCTION

The objective of the cell-fabrication effort during the period covered by this report has been to prepare cells having large area, thin substrates, and the highest possible efficiencies that can be reproduced in quantity. Originally the completed CdS cells were to be attached to a model of an inflatable torus sail to simulate a space power source. Near the end of the work RCA and ASD agreed that the CdS cells were not to be attached to the torus-sail model but that they were to be delivered as a separate item of the contract. Delays in obtaining equipment prevented this work from starting until the last part of June. In the three-months period since the start of work about 120 finished cells were processed, with a total active area of 300 square centimeters.

The total power output of these cells was initially measured at 500 mw. Since the start of the fabrication period, the cell area has increased consistently from 1.6 cm^2 to 19 cm^2. The area of one cell was increased to 44 cm^2. In addition, the thickness of the substrate was reduced by a factor of 6 to 0.010 inch and the cell weight reduced by a factor of 6 to .076 gm/cm^2.

One of the problems encountered is the deterioration of the electrical characteristics of the cells with storage time. Effort was spent on shelf life testing under various conditions, on investigation of the causes of deterioration, and on means for protecting cells against deterioration.

The procedure for preparing the cells is essentially the same as described in Section I of this report. Photoconductive CdS powder is evaporated in vacuum onto glass substrate. The substrate is coated with transparent, electrically conductive tin oxide, which serves as one electrode. The barrier layer is then formed on top of the CdS layer by firing finely divided copper in argon. Silver paint is then applied as the other electrode.

TECHNICAL DISCUSSION

1. RAW MATERIAL

All cells were fabricated from one lot of photoconductive CdS powder. No single crystal chips nor sintered cakes of CdS were used. The impurities or dopants in the raw material were therefore the same for all cells. The variations in conversion efficiency are due to factors other than impurities, principally CdS layer thickness and processing conditions and technique.

2. SUBSTRATES

The majority of the cells were made on Pyrex substrates coated with tin oxide as a backwall device. A few cells were made using a thin sheet of molybdenum as a frontwall device. The types and dimensions of the substrates and the weights of the finished cells are summarized in Table II. The areas given in this table represent total surface area of the substrate. Most of the surface is deposited with CdS, constituting the active cell area for computing cell conversion efficiency. Part of the substrate surface is used as one collecting electrode, though it does not play an active part in the conversion of energy. In the case of the molybdenum substrate, the entire surface is covered with CdS, but some of the area is also considered lost for energy conversion because of the application of silver stripes for the other electrode.

3. EQUIPMENT

Equipment used in the fabrication of cells is listed below:

a. Substrate degreaser

b. High vacuum evaporator and power supplies

c. Densichron densitometer*

d. Sim-Ply-Trol substrate temperature controller*

e. Brown Instrument evaporator temperature controller-recorder*

f. Hot plate

g. Muffle furnace and regulator*

h. Argon gas pressure regulator*

i. Balance

j. Brinkman Micro-manipulator*

*These items were purchased with government funds allocated to this contract.

TABLE II

SUMMARY OF TYPE AND DIMENSIONS OF SUBSTRATES AND WEIGHTS OF FINISHED CELLS

Group No.	Type of Material	Thickness (in.)	Area (cm^2)	Cell Weight (gm)	Weight/Cell Area (gm/cm^2)
1.	Pyrex	0.064	4.84	2.0189	0.4200
2.	Pyrex	0.064	6.45	2.6630	0.4130
3.	Pyrex	0.032	6.45	1.3760	0.2130
4.	Pyrex	0.017	6.45	0.6430	0.0995
5.	Pyrex	0.010	6.45	0.5956	0.0925
6.	Pyrex	0.064	25.80	10.3150	0.4000
7.	Pyrex	0.010	25.80	1.7371	0.0675
8.	Pyrex	0.064	61.99	26.5130	0.4100
9.	Molybdenum	0.003	6.45	0.4910	0.0760

k. Keithley electrometer

l. Ammeter

m. Leeds and Northrup potentiometer

n. Illuminator and filter

o. Glass wares

4. PROCESSES

The processes used in this work are basically those developed during photovoltaic material research. They consist of the following operations:

a. Substrate cleaning. In order to avoid introduction of impurities, to obtain adequate adherence of the CdS layer, and to eliminate pin holes, the substrate must be thoroughly cleaned. The procedure for cleaning glass substrates is first washing with a detergent using mechanical motion; second, rinsing with tap water and distilled water; third, soaking in distilled water for one hour, with the water changed every 15 minutes, rinsing with isopropyl alcohol; and fourth degreasing with isopropyl alcohol vapor for one hour. The procedure for cleaning metal substrate is the same, except for the addition of an etching step following the detergent washing and rinsing. For example, Molybdenum is etched in concentrated nitric acid for 7 minutes.

b. Evaporation and deposition of CdS layer. The CdS is deposited onto the substrate by evaporation of the CdS powder in vacuum. A procedure was evolved that would establish conditions for obtaining a layer suitable for the photovoltaic cell. First, a charge of 4 to 6 gm of CdS powder is placed in a tubular evaporator. The powder is rid of absorbed gas and high-vapor-pressure impurities by heating to between 950° and 1,000°C in vacuum for 20 minutes. The temperature is monitored by the temperature recorder.

After the evaporator is cooled to room temperature, the substrate assembly (substrates, mask, heater and holder) is mounted on a glass chimney over the evaporator. The substrate is then degassed at 175°C for one hour at a vacuum of 4×10^{-6}mm Hg. The CdS powder and evaporator are degassed again and the evaporator is allowed to reach the evaporation temperature of 1,000° to 1050°C in 15 minutes. The CdS deposition onto the substrate is then started and proceeds for 35 minutes, after which CdS layer on the substrate is allowed to cool to below 75°C. The CdS layer is examined for pin holes after removal from the evaporator.

c. Formation of barrier layer and testing. After the CdS layer has been inspected, it is prepared for formation of the barrier layer by etching in an 18-percent HCl solution for 5 seconds, and rinsing with distilled water. Finely divided copper is then applied over the CdS layer at 65°C. The copper layer is heated to 300°C in 3 minutes in argon atmosphere. After the cell has cooled to room temperature, excess copper is removed from the black barrier layer. Electrodes are then formed by applying silver paint over the barrier layer and on the edges of the substrate. The completed cell is tested by measuring the open-circuit voltage, the short-circuit current and the current-voltage characteristic, under a calibrated tungsten light source, using a water filter.

5. POWER AND ELECTRICAL CHARACTERISTICS OF CELLS

The electrical characteristics, maximum power and conversion efficiency of each cell were determined immediately after fabrication. The open-circuit voltage usually ranges from 0.41 to 0.52 v. The short-circuit current varies with cell size from 15 ma for the small cell size to 135 ma for the large cell. In addition, there are variations among cells of the same size due to processing factors. Total power of each cell also increases with area, and varies from 2 mw to 26 mw. Conversion efficiency, n, is calculated from the formula:

$$n = \frac{\text{Power output (mw)} \times 100}{\text{Area (cm}^2\text{)} \times 100 \text{ mw/cm}^2 \text{ (energy input)}}$$

and varies from 0.5 to 3.5 percent. These data are shown in Table III, which also includes the total power and area of the cells. Typical current-voltage curves are shown in Figure 14, 15, 16, and 17. One curve is shown for each of the four sizes of cells.

As seen from the data, the conversion efficiency decreases with the cell area. The current-voltage curve also becomes less rectangular as the area increases. The decrease in efficiency is believed to result at least partly from the increase in the sheet resistance of the tin-oxide coating on the glass substrate. To confirm this belief, the sheet resistance of the tin-oxide coated glass was measured from the center to the edge of each of the four sides of the cells. (The length of the electrode parallel to the edge of the cell is 0.5 centimeter.) These data are shown in Table IV. Figure 18 is a plot of the average efficiency measured versus sheet resistance in ohm-cm^2. For comparison, a similar curve for a GaAs cell, taken by J.J. Wysocki[9] is also shown here. The actual quantities are different, but the similarity in the shape of the curve is evident, indicating qualitative agreement.

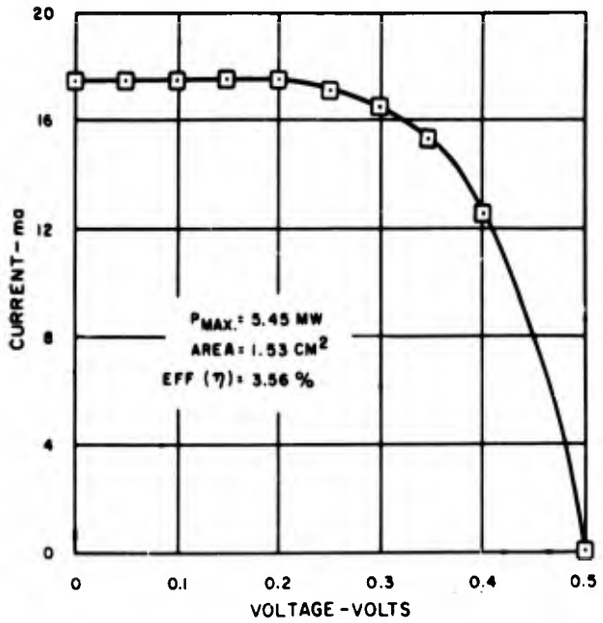

Figure 14. Current-Voltage Characteristic of CdS Photovoltaic Cell #15-2

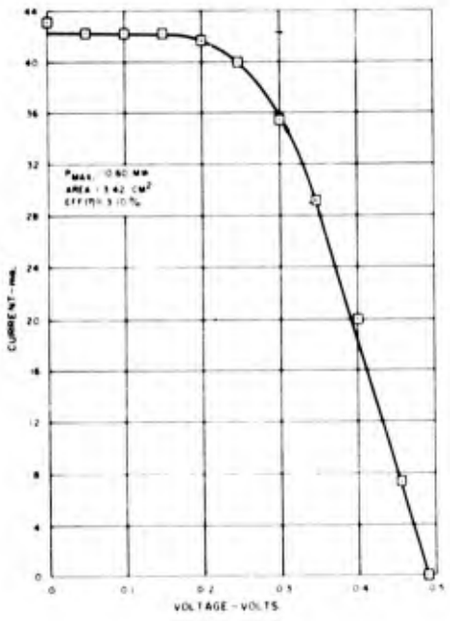

Figure 15. Current-Voltage Characteristic of CdS Photovoltaic Cell #76-4

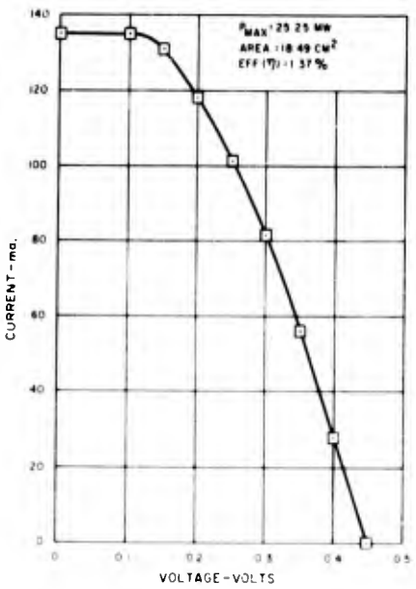

Figure 16. Current-Voltage Characteristic of CdS Photovoltaic Cell #81

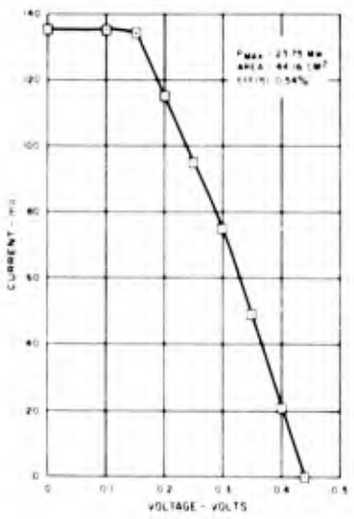

Figure 17. Current-Voltage Characteristic of CdS Photovoltaic Cell #83

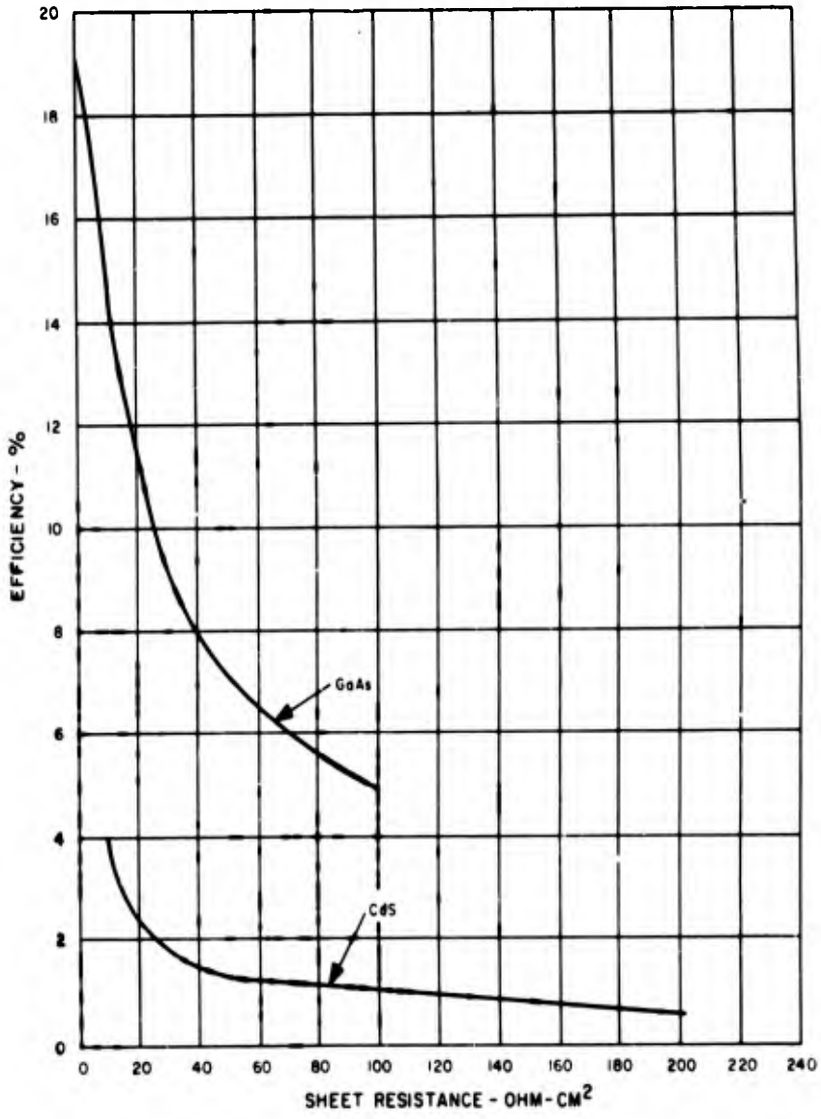

Figure 18. Effect of Sheet Resistance on Conversion Efficiency of CdS and GaAs Photovoltaic Cells

TABLE III

ELECTRICAL CHARACTERISTICS, POWER, AND EFFICIENCY OF CdS PHOTOVOLTAIC CELLS

Cell No.*	Cell Thickness (in)	Active Area (cm^2)	$I_{s.c.}$ (ma)	$V_{o.c.}$ (v)	Power (mw)	Efficiency (%)	Cell No.*	Cell Thickness (in)	Active Area (cm^2)	$I_{s.c.}$ (ma)	$V_{o.c.}$ (v)	Power (mw)	Efficiency (%)
06-2	.060	1.37	14.5	0.44	2.00	1.46	63-3	.060	3.33	37.6	0.47	7.50	2.25
10-3	.060	1.62	19.5	0.50	4.25	2.62	63-4	.060	3.42	38.5	0.47	8.60	2.51
11-1	.060	1.45	8.0	0.48	0.52	0.36	64-1	.060	3.15	30.0	0.46	7.40	2.35
13-1	.060	1.52	12.0	0.51	2.55	1.68	64-2	.060	3.11	32.0	0.48	6.50	2.09
14-2	.060	1.50	20.0	0.52	4.95	3.30	64-3	.060	3.25	38.0	0.45	7.50	2.30
14-3	.060	1.66	20.0	0.55	4.20	2.53	64-4	.060	2.95	26.0	0.42	4.00	1.36
15-1**	.060	1.57	25.7	0.52	6.72	4.27	65-1	.030	3.06	12.2	0.50	2.88	0.94
15-2	.060	1.53	17.5	0.50	5.45	3.56	65-2	.030	3.32	46.0	0.46	9.75	2.94
17-3D	.060	1.45	17.5	0.47	2.40	1.65	65-3	.030	3.06	14.2	0.49	4.34	1.42
18-1	.060	1.65	24.0	0.45	5.25	3.18	65-4	.030	3.24	42.5	0.46	9.13	2.82
20-1	.060	1.68	21.5	0.49	4.05	2.41	66-1	.030	3.15	43.0	0.46	7.50	2.38
24-1	.060	1.35	17.6	0.45	2.80	2.08	66-2†	.030	3.24	45.0	0.46	8.30	2.56
26-2	.060	1.54	13.0	0.48	3.00	1.95	66-4	.030	3.24	46.5	0.47	8.63	2.66
30-1	.060	1.70	19.0	0.47	3.05	1.79	67-1	.030	2.89	22.5	0.37	2.60	0.90
30-3	.060	1.36	11.0	0.27	0.90	0.66	67-2†	.030	2.55	32.5	0.43	5.00	1.96
30-4	.060	1.68	20.0	0.46	4.63	2.76	67-3	.030	2.89	35.5	0.44	5.20	1.80
30-4**	.060	1.33	19.0	0.45	3.50	2.63	67-4	.030	3.06	41.0	0.41	6.25	2.04
51-4	.030	2.72	31.4	0.43	5.80	2.13	69-1	.017	3.42	26.0	0.49	3.88	1.14
55-2	.060	3.02	22.5	0.46	4.40	1.46	69-2	.017	3.24	29.0	0.48	7.05	2.18
60-1	.060	3.11	16.0	0.46	3.45	1.11	69-3†	.017	3.15	29.5	0.45	5.50	1.75
							71-2	.017	3.24	29.0	0.50	7.20	2.22
60-4	.060	3.24	17.5	0.48	4.50	1.39	71-4	.017	3.24	27.5	0.48	6.60	2.04
61-2**	.060	2.97	13.5	0.31	2.85	0.96	72-3	.017	3.33	36.5	0.48	8.70	2.61
61-3***	.060	3.06	16.5	0.47	3.31	1.08	73-1	.017	3.33	18.0	0.27	0.90	0.27
61-4	.060	3.98	15.5	0.23	5.48	1.84	73-2	.017	3.15	32.0	0.44	6.60	2.10
63-1	.060	3.22	40.0	0.48	7.60	2.36	73-3	.017	2.72	31.5	0.41	4.50	1.65
63-2	.060	2.89	35.0	0.48	7.10	2.46	73-4	.017	3.24	20.0	0.34	2.04	0.63
							74-4	.017	3.06	38.0	0.46	6.70	2.19

TABLE III

ELECTRICAL CHARACTERISTICS, POWER, AND EFFICIENCY OF CdS PHOTOVOLTAIC CELLS (CONT)

Cell No.*	Cell Thickness (in)	Active Area (cm^2)	$I_{s.c.}$ (ma)	$V_{o.c.}$ (v)	Power (mw)	Efficiency (%)	Cell No.*	Cell Thickness (in)	Active Area (cm^2)	$I_{s.c.}$ (ma)	$V_{o.c.}$ (v)	Power (mw)	Efficiency (%)
74-1A	.017	3.24	35.5	0.48	8.40	2.59	77-2	.012	3.06	33.5	0.49	8.50	2.78
74-2A	.017	3.42	44.0	0.48	8.10	2.37	79	.060	18.49	117.0	0.47	21.20	1.15
74-3A	.017	3.24	42.5	0.47	7.00	2.16	80	.060	17.64	123.0	0.50	23.25	1.32
74-4A	.017	3.33	40.5	0.46	8.10	2.43	81	.060	18.49	135.0	0.45	25.25	1.37
75-3	.017	2.72	42.5	0.47	9.00	3.31	83	.060	44.16	135.0	0.44	23.75	0.54
75-4	.017	3.15	43.5	0.45	8.90	2.82	84	.060	18.50	136.0	0.46	25.50	1.38
76-1	.060	3.42	40.5	0.46	8.85	2.59	85-2††	.003	2.89	9.0	0.36	1.04	0.36
76-2	.060	3.42	39.0	0.49	9.70	2.84	88-1††	.003	1.80	17.8	0.41	2.62	1.45
76-4	.060	3.42	43.0	0.49	10.60	3.10	88-2††	.003	1.68	14.0	0.37	1.50	0.89
							89	.010	19.36	110	0.41	17.60	0.91
									316.63 (Total)			504.12 (Total)	

* The first 2 digits represents the number of an evaporation run.
The next digit represents the number of a particular cell made from that evaporation run.
Runs 01 through 78 and runs 85 through 88 produced 4 CdS layers per evaporation.
Runs 79 through 84 and run 89 produced 1 CdS layer per evaporation.

** Samples for baking at 300°C.

*** Sample mounted in vacuum tube.

† Samples covered with polystyrene.

†† Samples deposited on molybdenum.

TABLE IV
SHEET RESISTANCE OF TIN-OXIDE COATED GLASS SUBSTRATES

Substrate Size (in.)	Distance Center to Edge (cm)	Resistance (ohms)	Area Where Resistance Is Measured (cm^2)	Resistance Square (ohm-cm^2)
1 x 3/4	1.00	16	0.500	8.00
1 x 1	1.27	18	0.635	11.43
2 x 2	2.54	46	1.270	58.42
3.5*	4.50	90	2.250	202.50

* Diameter; this substrate is round.

Another experiment was performed to show the effect of the sheet resistance. The current-voltage characteristic, power, and efficiency of the typical 2 x 2 inch cell shown in Figure 19 were taken in the normal manner.

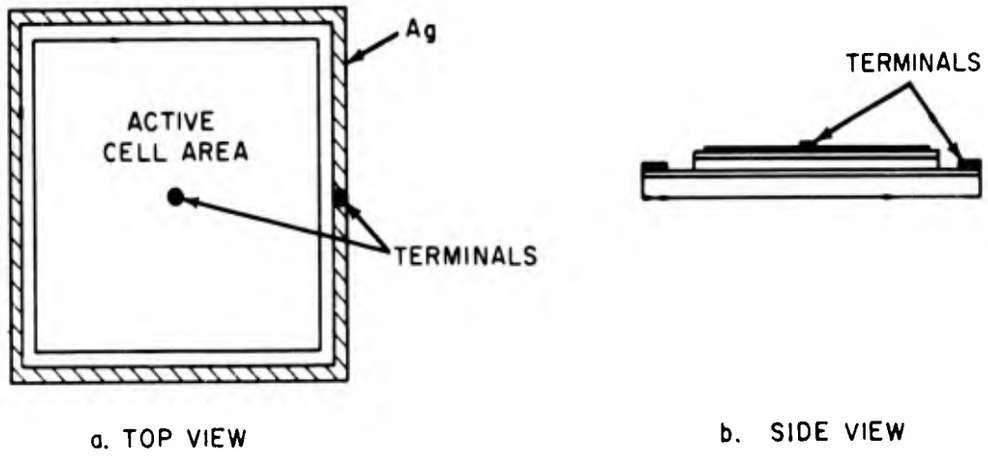

Figure 19. Typical 2 x 2-in. CdS Cell

As shown, both the active cell area and the four edges (1/16 inch wide) are printed with silver. Electrical contacts are made at the center of the active area and at a point on one edge. This cell showed a maximum power of 21.3 mw and an efficiency of 1.05 percent after 10 days storage in a dessicator. The silver along three of the four edges was then removed. Current-voltage curves were taken with the electrical contact to the active cell area relocated to seven different points. The other contact remained at one edge of the cell. The maximum power at all seven points in the active cell area, dropped to between 7.5 and 8.0 mw, and efficiency dropped to 0.37 percent. Furthermore, measurements were made on only selected portions of the active area, with the rest of the area blanked out from the light source. These data are shown in Table V.

TABLE V

MEASUREMENTS OF POWER AND EFFICIENCY OF CELL #81 WITH ELECTRODES AT DIFFERENT LOCATIONS AND FOR DIFFERENT CELL AREAS

Cell Edge Electrode	Cell Area (cm^2)	$I_{s.c.}$ (ma)	$V_{o.c.}$ (V)	$P_{max.}$ (mw)	N (%)
4 sides	20.25	119	0.45	21.3	1.05
1 side	20.25	54	0.45	8.0	0.39
1 side	20.25	53	0.44	8.0	0.39
1 side	20.25	53	0.44	7.75	0.38
1 side	20.25	53	0.44	7.50	0.37
1 side	20.25	51	0.43	7.50	0.37
1 side	20.25	52	0.43	7.75	0.38
1 side	20.25	52	0.43	7.75	0.38
1 side	6.45 (next to edge electrode)	41	0.44	7.30	1.13
1 side	5.08 (next to edge electrode)	39	0.44	7.20	1.42
1 side	1.56 (next to edge electrode)	17	0.43	3.40	2.18
1 side	4.00 (furthest lower corner)	16	0.37	1.55	0.39
1 side	4.00 (furthest upper corner)	15	0.36	1.40	0.35

The effect of sheet resistance on conversion efficiency of large area-cells is clearly shown. Because of its dominant role, every effort will be made to reduce this resistance.

Other factors that influence the conversion efficiency are the thickness, structure, and chemical composition of the CdS layer; the substrate temperature during deposition; the evaporation temperature and pressure; the deposition rate; the contact between the copper and the CdS layers; the conversion temperature, atmosphere and time of the copper or barrier layer; and the types of electrode contacts and electrical leakage between electrodes. The thickness of the CdS layers during the initial and some subsequent evaporations was in the 5 to 10-micron range, and the efficiencies of these cells were very low. CdS layer thicknesses between 20 and 30 microns usually give higher cell efficiencies. In one evaporation (run 16) the substrate temperature was below 50° C and the CdS layers appeared very dark in color instead of being brown. This is attributed to a change in the chemical composition of the layer. None of the four cells from this run produced any current-voltage reading.

The deposition rate in many of the early evaporations was low because of lower evaporation temperature. These cells also gave low electrical readings and showed pin holes in the CdS layer. Later evaporations were carried out at higher temperature (approximately 1000°C) and in shorter time (approximately 35 minutes). In one case, the copper layers of two cells were heated to 300°C in argon for 45 minutes. No photovoltaic effect was observed from these cells. Several cells with the copper layer heated at 100°C in air also gave low efficiency. All of the foregoing factors will be studied further in order to optimize the processing conditions. Effects of impurities and dopants will also be studied.

6. LIFE TESTS

The power and efficiency of CdS photovoltaic cells decay with time during storage in room air. To determine some means of protection against decay preliminary studies were made of the degree of decay and the possible causes including storage conditions. This work was concerned with shelf life test only. No operating life tests were performed.

a. Degree of Decay in Air. Five cells, 13-1, 14-2, 15-1, 26-2 and 30-4, were taken out of the Drierite Dessicator (usual storage) and left on the laboratory bench. These cells were mounted on small plastic boxes with adhesive tape, and daily readings were taken of the current-voltage characteristics. The results, presented in Table VI, indicate that the initial rate of decay is high and gradually decreases, showing a very gradual drop after 90 days. There seem to be two types of decay. In one case, only the current drops, but the

TABLE VI
DECAY OF ELECTRICAL CHARACTERISTICS OF CdS CELLS STORED IN AIR

Cell No.	Days Storage	$I_{s.c.}$ (ma)	$V_{o.c.}$ (v)	$V_{max.\ p.}$ (v)	Power (mw)	Eff. (%)	Decay (%)
13-1	0	12.0	0.51	0.25	2.55	1.678	--
	33*	4.4	0.51	0.20	0.42	0.276	83.6
	40	4.6	0.54	0.20	0.56	0.368	78.1
	46	4.3	0.50	0.25	0.57	0.375	77.7
	54	5.0	0.50	0.25	0.81	0.533	68.3
	81	5.0	0.50	0.25	0.88	0.579	65.5
	94	5.5	0.51	0.30	0.96	0.631	62.5
14-2	0	20.0	0.52	0.30	4.86	3.20	--
	33*	11.0	0.52	0.25	2.00	1.32	58.8
	40	9.1	0.53	0.25	1.55	0.99	69.1
	46	7.0	0.48	0.25	1.31	0.86	73.2
	54	7.0	0.49	0.30	1.50	0.99	69.1
	81	6.0	0.49	0.30	1.35	0.89	72.2
	94	5.2	0.48	0.30	1.20	0.79	75.4
15-1	0	25.6	0.50	0.30	6.72	4.27	--
	5*	23.8	0.53	0.30	6.00	3.83	10.3
	81**	7.5	0.30	0.20	0.60	0.38	91.2
	94	6.2	0.28	0.15	0.51	0.32	92.5
26-2	0	13.0	0.48	0.30	3.00	2.07	--
	17*	7.2	0.51	0.25	1.13	0.78	62.3
	24	5.2	0.51	0.25	0.78	0.54	73.8
	31	4.5	0.50	0.25	0.88	0.61	70.5
	66	3.5	0.48	0.25	0.70	0.48	76.8
30-4	0	20.0	0.47	0.30	4.50	2.90	--
	17*	5.0	0.25	0.15	0.30	0.19	93.5
	24	3.8	0.22	0.10	0.35	0.22	92.5
	66	3.3	0.27	0.10	0.15	0.09	97.0

* In Drierite Desiccator during part of the storage time.
** In air most of the storage time.

open-circuit voltage remains practically constant. In the other, there is a drop in both the current and open-circuit voltage and the maximum power point shifts toward the lower voltages, i.e., the current-voltage curve becomes less rectangular.

b. Storage Under Vacuum. In order to determine the environmental effect, six cells were stored in a vacuum. Two of them, 59-4 and a 2 x 2-inch cell, were put in a glass tube which was evacuated to a 10-micron pressure and sealed off. The electrical connections passed through the glass. Four cells, put in a vacuum system with a pressure of 10-20 microns, were exposed to air during the daily electrical measurements. In order to see if there would be any recovery under vacuum, only three of the six cells used were older cells. The other three were new cells. The results are shown in Table VII.

c. Effect of Polystyrene Coating. As a protective measure, polystyrene coating was applied to three new cells by the glow-discharge method. This method was preferred over others, because it is done in vacuum and thereby removes some of the adsorbed gases from the cell surface. This method also reduces contamination by solvents and other impurities. By controlling the pressure, current, and deposition time, a coating was produced whose thickness was estimated to be on the order of 20 microns. Electrical wires were attached to the cells with silver paste before the coating was applied. The electrical readings are shown in Table VIII.

d. Effect of Drying Agent. In order to differentiate between the effect on decay of the moisture and oxygen components in the air, two cells were placed in separate plastic boxes containing some phosphorus pentoxide. The boxes were then sealed with adhesive tape. Electrical measurements were made on one cell by means of wires which passed through the sealed box. Readings on the other cell were taken by removing it from the box. The data are shown in Table IX.

e. Effect of Reheating. Two experiments were conducted to investigate the possibility of effecting a recovery of cell efficiency by removing adsorbed gases or moisture from the cell. In one experiment, several cells, whose efficiencies had already decayed to very low values were reheated in argon to 300°C in 3 minutes. One cell, 61-2, showed almost complete recovery when it was heated after storage in air. The other cells did not show a marked response to heating. The data for this experiment are presented in Table X.

In the second experiment, the silver electrodes of several old cells were removed with solvent. The cells were dried and new silver electrodes were affixed. The cells were then tested. After testing, these cells were heated in argon to 300°C in 3 minutes and tested again. Data for the second experiment are given in Table XI.

TABLE VII

DECAY OF ELECTRICAL CHARACTERISTICS OF Cds CELLS STORED UNDER VACUUM

Cell No.	Storage Condition	Days Storage	$I_{s.c.}$ (ma)	$V_{o.c.}$ (v)	$V_{max.\ p.}$ (v)	Power (mw)	Eff. (%)	Decay (%)
59-4	----	0	17	0.46	0.25	3.45	1.065	----
	Drierite Desiccator	30	14	0.44	0.30	2.76	.852	20.2
	Vacuum Tube	36	11	0.42	0.25	2.10	.648	39.2
	"	46	11	0.40	0.25	2.10	.648	39.2
	"	61	11	0.42	0.25	2.10	.648	39.2
	"	81	11	0.42	0.25	2.25	.695	34.7
	"	108	11	0.40	0.25	2.25	.695	34.7
2" x 2" cell	----	0	132	0.46	0.25	25.00	1.390	----
	Air	5	52	0.34	0.15	5.40	.300	78.7
	Vacuum Tube	5	50	0.35	0.15	5.30	.294	78.9
	"	10	50	0.34	0.20	5.64	.314	77.5
	"	15	50	0.34	0.15	3.93	.218	84.5
	"	20	48	0.33	0.15	5.14	.286	79.5
63-4	----	0	38.4	0.47	0.30	8.64	2.450	----
	Drierite Desiccator	30	25.7	0.35	0.20	3.42	0.970	60.5
	Vacuum System	35	25.2	0.34	0.20	3.40	0.965	60.6
	"	45	25.0	0.33	0.20	3.10	0.880	64.1
	"	60	24.0	0.32	0.20	2.92	0.828	66.3
72-3	----	0	36.5	0.48	0.30	8.70	2.61	----
	Vacuum System	3	34.5	0.46	0.30	7.20	2.16	17.2
	"	5	32.3	0.47	0.30	7.50	2.25	13.8
	"	7	33.0	0.47	0.30	6.90	2.07	20.7
	"	11	31.0	0.46	0.30	7.10	2.13	18.4
74-1A	----	0	35.5	0.48	0.30	8.40	2.59	----
	Vacuum System	3	32.0	0.47	0.30	7.05	2.18	15.8
	"	5	31.0	0.47	0.30	7.50	2.31	10.8
	"	7	31.5	0.45	0.30	6.75	2.08	19.7
	"	11	30.2	0.46	0.30	6.78	2.09	19.3
75-3	----	0	42.5	0.47	0.30	9.00	3.31	----
	Vacuum System	3	38.5	0.46	0.25	6.13	2.25	32.0
	"	5	39.0	0.47	0.30	9.00	3.31	0
	"	7	38.5	0.45	0.30	8.00	2.94	11.2
	"	11	37.0	0.46	0.30	8.16	3.00	9.37

TABLE VIII
EFFECT OF POLYSTYRENE COATING ON DECAY OF CdS CELLS

Cell No.	Days	$I_{s.c.}$ (ma)	$V_{o.c.}$ (v)	$V_{max.\ p.}$ (v)	Power (mw)	Eff. (%)	Decay (%)
66-2	0	35.0	0.47	0.30	7.2	2.36	-
	1	35.0	0.47	0.30	7.2	2.36	0
	2	33.0	0.49	0.30	7.5	2.45	0
	3	33.5	0.47	0.30	6.6	2.16	8.47
	4	29.5	0.46	0.30	6.0	1.96	16.95
	7	26.0	0.45	0.30	5.3	1.73	26.70
	9	24.5	0.46	0.30	5.2	1.70	28.00
	14	20.5	0.45	0.30	4.1	1.34	43.20
	30	15.2	0.42	0.30	2.9	0.95	59.75
67-2	0	22.5	0.44	0.25	4.0	1.23	-
	1	21.0	0.44	0.25	3.6	1.11	9.76
	2	20.0	0.42	0.25	3.1	0.96	21.90
	3	16.0	0.40	0.25	2.3	0.71	42.30
	7	12.0	0.37	0.25	1.4	0.40	67.50
	10	8.0	0.32	0.20	0.66	0.20	83.80
	30	2.0	0.15	-	-	-	-
69-3	0	30.0	0.39	0.25	4.8	1.65	-
	1	31.0	0.42	0.25	5.5	1.90	0
	2	25.5	0.40	0.25	3.8	1.31	20.6
	5	20.0	0.34	0.20	2.7	0.83	49.7
	7	17.0	0.33	0.20	2.1	0.66	60.0
	10	13.5	0.28	0.15	1.3	0.45	72.7
	22	3.0	0.08	-	-	-	-

TABLE IX

EFFECT OF DRYING AGENT P_2O_5 ON DECAY OF CdS CELLS

Cell No.	Days	$I_{s.c.}$ (ma)	$V_{o.c.}$ (v)	$V_{max.p.}$ (v)	Power (mw)	Eff. (%)	Decay (%)
87	0	44	0.34	0.20	4.6	.356	--
	3*	31.6	0.26	0.15	2.6	.202	43.3
	4**	34.0	0.27	0.15	2.9	.225	36.8
	8	33.0	0.25	0.15	2.6	.202	43.3
	16	34.5	0.27	0.15	3.0	.232	34.8
81	0	135	0.45	0.25	25.25	1.25	--
	11*	119	0.45	0.25	21.3	1.05	16.0
	12***	53	0.44	0.25	8.0	0.39	68.8
	15***	53	0.45	0.25	7.8	0.38	69.5
	21	54	0.45	0.25	8.3	0.41	67.1

* In Drierite desiccator.

** Electrical wires attached through box.

*** This cell had the silver-paint electrode on only one edge.
Refer to the discussion of Sheet resistance which appears elsewhere in this section.

TABLE X
EFFECT OF HEATING ON DECAY OF CdS CELLS

Cell No.	Heating	$I_{s.c.}$ (ma)	$V_{o.c.}$ (v)	$V_{max.p.}$ (v)	Power (mw)	Eff. (%)	Recovery (%)
61-2	Initial	17	0.43	0.30	2.85	.960	--
	After decay Before Heating	7.7	0.06	0.15	0.09	.030	
	After Heating	14.5	0.35	0.20	2.04	.687	70.60
	Storage	9.4	0.25	0.15	0.48	.162	
	Heating Again	14.0	0.32	0.20	2.00	.674	64.25
20-2D	Initial	14.5	0.46	0.25	1.95	1.370	
	After decay Before Heating	3.5	0.20	0.10	0.23	.162	
	After Heating	3.7	0.36	0.25	0.63	.444	23.36
15-1	Initial	25.7	0.52	0.30	6.72	4.27	
	After decay Before Heating	5.6	0.27	0.15	0.41	.261	
	After Heating	8.3	0.23	0.10	0.55	.350	2.22
57-1	Initial	16.0	0.46	0.25	2.75	1.222	
	After decay Before Heating	11.7	0.44	0.30	2.28	1.013	
	After Heating	10.0	0.42	0.25	1.70	.755	--

TABLE XI
EFFECT OF HEATING AND NEW ELECTRODE CONTACTS
ON DECAY OF CdS CELLS

Cell No.	Electrodes	$I_{s.c.}$ (ma)	$V_{o.c.}$ (v)	$V_{max.\ p.}$ (v)	Power (mw)	Eff. (%)
15-1	Initial	25.7	0.52	0.30	6.72	4.27
	Old	8.5	0.27	0.15	0.66	0.42
	New	8.5	0.40	0.25	1.70	1.08
	After Heating	7.6	0.39	0.25	1.53	0.97
20-2D	Initial	14.5	0.46	0.25	1.95	1.37
	Old	3.5	0.38	0.25	0.65	0.456
	New	2.6	0.33	0.20	0.44	0.309
	After Heating	2.9	0.35	0.25	0.58	0.408
30-4	Initial	20.0	0.46	0.30	4.63	2.76
	Old	4.0	0.13	0.10	0.16	0.095
	New	3.0	0.26	0.15	0.33	0.196
	After Heating	2.5	0.28	0.20	0.34	0.202
57-1	Initial	16.0	0.46	0.25	2.75	1.222
	Old	9.8	0.43	0.25	1.65	0.734
	New	7.6	0.40	0.25	1.40	0.622
	After Heating	6.8	0.37	0.25	1.25	0.555

f. Summary and Discussion of Life Test Results. The decay of the conversion efficiency of CdS photovoltaic cells with time is rather severe when the cells are exposed to atmosphere. Test data showed that there are two classes of decay. In one class, the open-circuit voltage remains stable; only the current decreases with time. In the other, both the open-circuit voltage and current decrease.

Tests indicate that storage under vacuum and storage in desiccated atmosphere can arrest the decay, and point to moisture as the offending component in the atmosphere. The slight decay observed during these experiments is believed to have occurred during measurements when the cells were exposed to air. It is interesting to note that there was no decay in the open-circuit voltage when the cells were placed under vacuum or when a drying agent was used. Tests in which a polystyrene coating was used indicated that initial decay was slowed, as shown in Figure 20. During these tests it was observed that cracks developed in the polystyrene coating and subsequently the decay became as rapid as during exposure to atmosphere.

Results of the heating experiment are inconclusive, except that one cell showed substantial recovery. Tests involving the use of a new silver electrode were also inconclusive. Further work is needed to clarify the results of both tests.

There are possibly two elements which constitute cell decay. One is related to the change in the number of carriers and the field at the barrier layer. The other is related to the change in contact resistance at the junction. This resistance, coupled with the leakage paths between electrodes, produces the decay in open-circuit voltage. The leakage paths are formed by the action of condensed moisture on the glass surface, which dissolves some surface salt and forms an electrolyte. Figure 20 shows the typical decay curves of CdS cells under various conditions. A decay curve (efficiency versus contact resistance at the junction) for GaAs[9] is also shown in Figure 20. The similarity between the shapes of the curves seems to indicate that changes in contact resistance might be the cause for the decay of conversion efficiency in CdS cells. This avenue of investigation will require further effort before conclusive results are obtained.

SUMMARY AND CONCLUSIONS RELATING TO CdS CELL FABRICATION

During the fabrication program cells were made on progressively thinner substrates, and over larger areas, although efficiencies for very large areas were low. Further efforts are required, however to reduce the sheet resistance for the very large area cells and to devise means of eliminating or preventing the decay of the conversion efficiency. The use of doping materials and of improving processing parameters and techniques is also necessary to enhance the initial conversion efficiency. Operating life tests must be performed to determine the reliability of the cells.

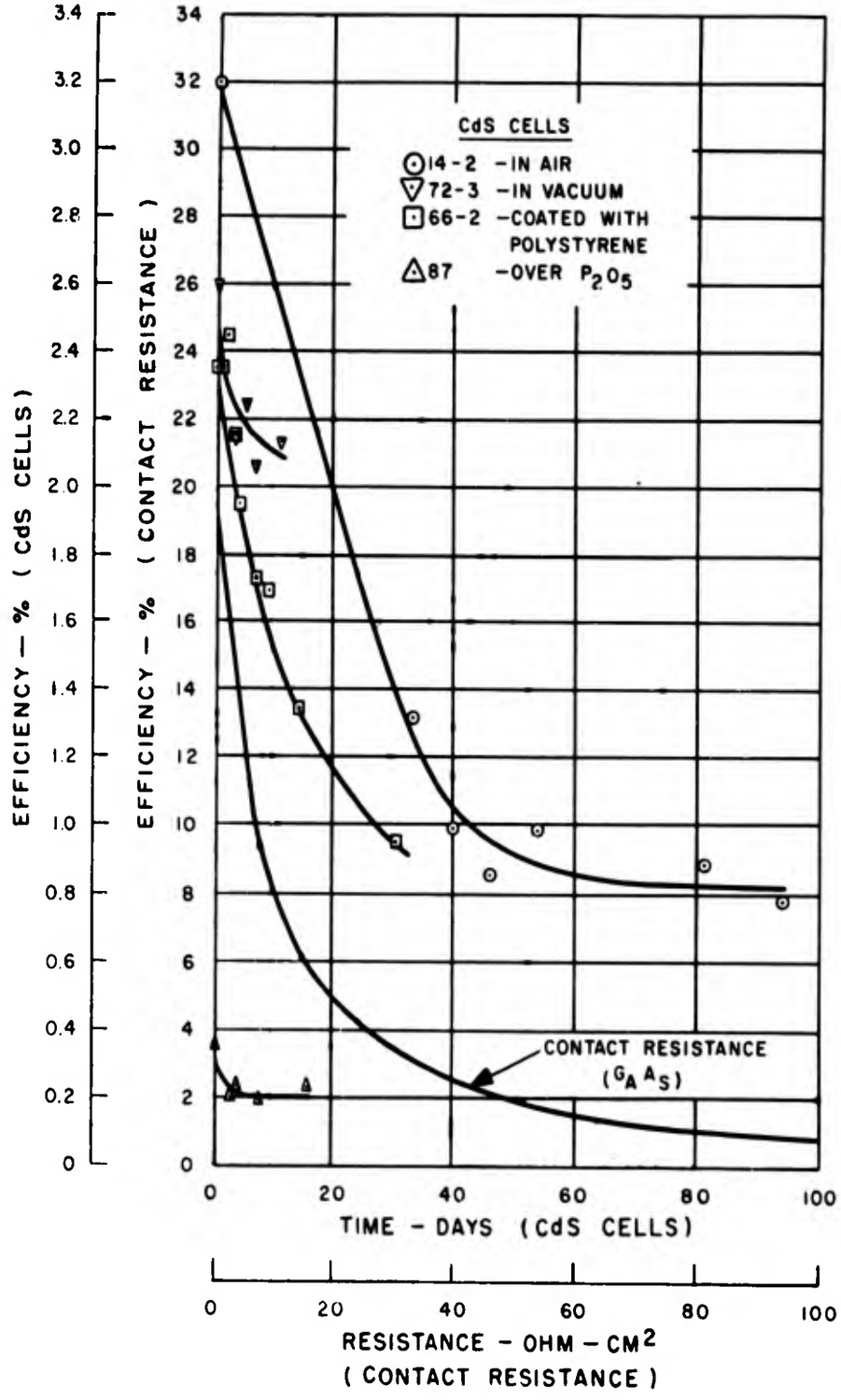

Figure 20. Decay of Conversion Efficiency of CdS Photovoltaic Cells

IV. FABRICATION OF ARRAY MODEL STRUCTURES

A. TORUS SAIL PROTOTYPE ARRAY

INTRODUCTION

The objective of a portion of the study program was to develop optimum structures and techniques for use in oriented solar cell arrays. Such arrays must comply with the following criteria.

a. Meet all reliability and environmental conditions.

b. Have a high power-to-weight ratio (watts output/pound of array).

c. Have a low area density (pounds of array/array area).

d. Have a high area-to-volume ratio (array area (ft^2)/stored array volume (ft^3)).

The torus sail promises to offer the optimum inflatable solar cell array, particularly in the power range above 1 kw where weight densities less than 0.04 lb/ft^2 (for the sail only) are well within present state-of-the-art techniques. The torus sail inherently achieves large ratios of deployed area to stowed volume and weight, and provides adequate structural integrity and system reliability for space applications. Deployment sequences are involved which would not produce intolerable change in space stabilization and orientation. A 100 ft^2 deployed array, for example, supplying 1 kw of power at present silicon cell efficiencies (10 watts/ft^2) can be contained in a frustum cone section approximately 1-1/2 feet high with a base diameter of 3 feet. Functional experimental and analytical studies conducted at RCA have provided further engineering support data on the feasibility of an array of this nature. Figure 21 illustrates the operation of a model torus array designed in connection with these studies. Figures 22, 23 and 24 give design data for this array. The torus sail was thus selected as one of the deliverable solar-cell array prototype models to demonstrate high density packaging, lightweight support structure and simplified reliable erecting techniques.

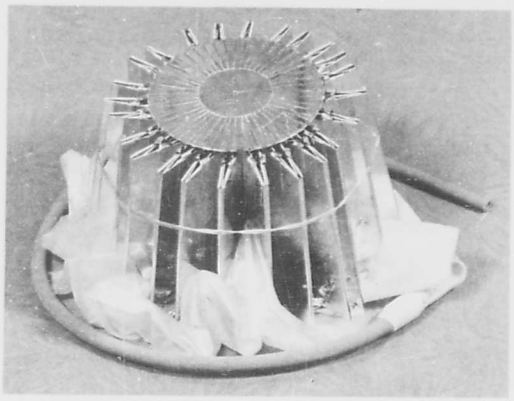

Model of a Solar-Cell Array, Folded

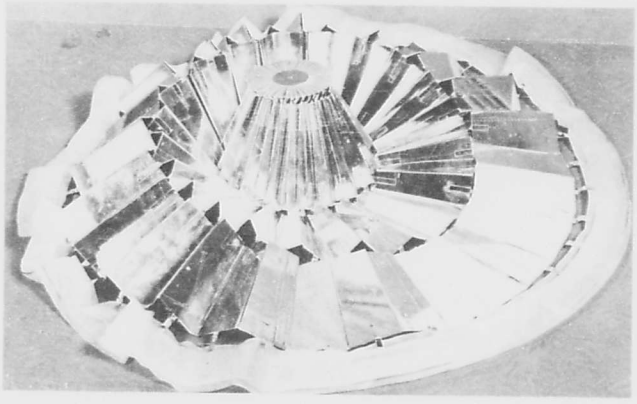

Model of a Solar-Cell Array, Partially Unfolded

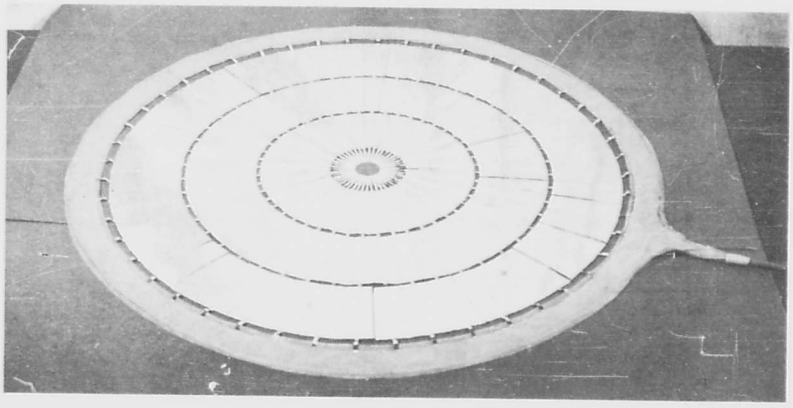

Model of a Solar-Cell Array, Fully Extended

Figure 21. Operation of Model Solar-Cell Array

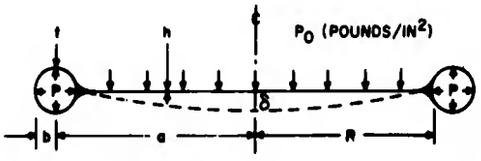

VALID FOR $b/R \geq 1.0$ $\quad \mu = 0.3$ in/in $\quad \sigma_R h \leq \frac{3\pi E b^3 t}{a^3}$

MEMBRANE TENSILE LOADING ONLY

NOMENCLATURE

h	= MEMBRANE THICKNESS (IN.)	P	= TORUS PRESSURE (psi)
P_0	= UNIFORM PRESSURE DISTRIBUTION (psi)	σ_t	= TANGENTIAL STRESS (psi)
σ_R	= RADIAL STRESS (psi)	P_R	= REFERENCE PRESSURE (psi)
t	= TORUS THICKNESS (IN.)	a	= AVERAGE TORUS RADIUS (IN.)
b	= TORUS CROSS SECTIONAL RADIUS (IN.)	R	= SAIL OUTER RADIUS (IN.)
δ	= SAIL DEFLECTION WITH ZERO SLOPE AT TORUS (IN.)		
E	= MODULUS OF ELASTICITY (psi)		

Figure 22. Solar-Collector Design Analysis: Terminology

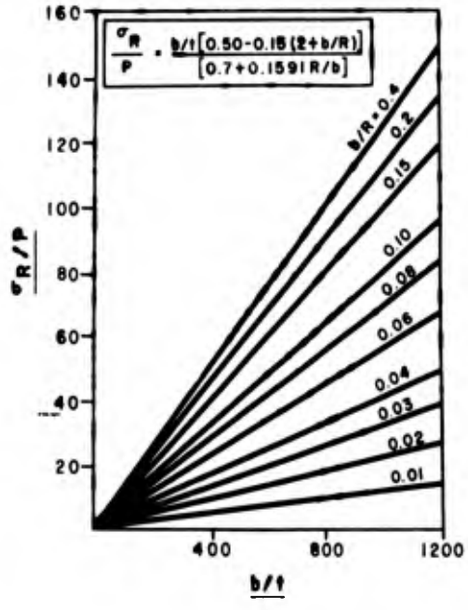

Figure 23. Solar-Collector Design Analysis: Plot of σ_R/p Vs b/t

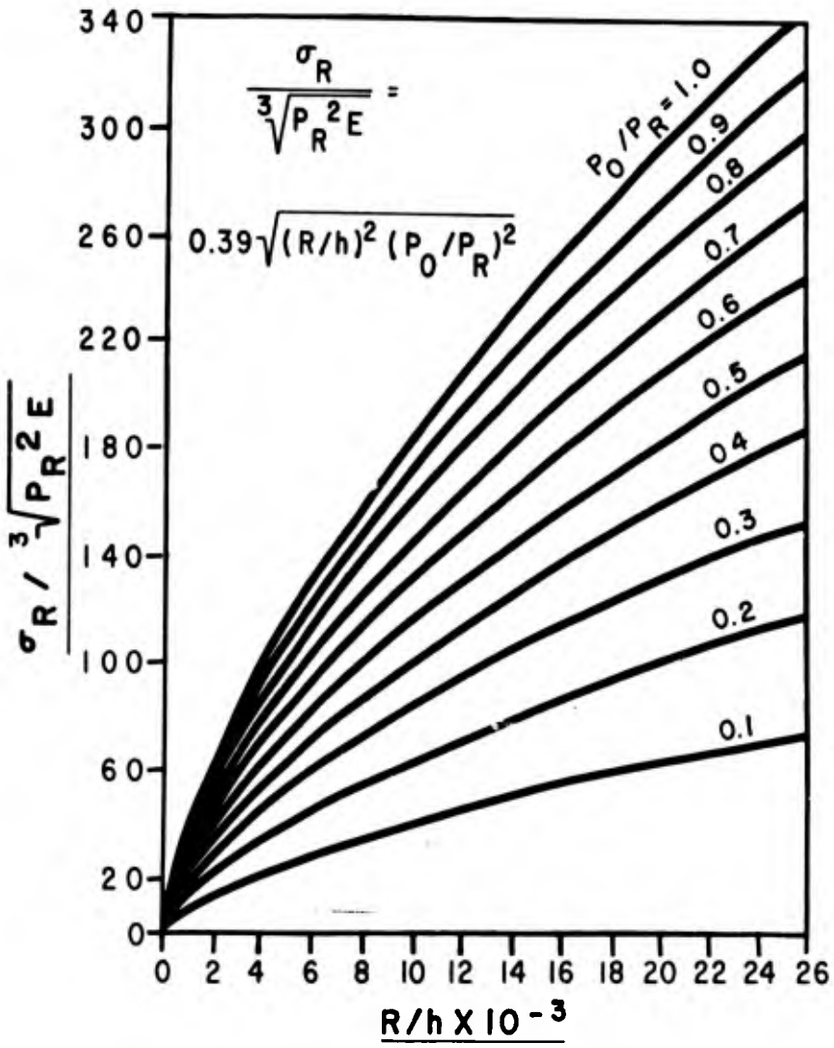

Figure 24. Solar Collector Design Analysis: Plot of $\sigma_R / \sqrt[3]{P_R^2 E}$

TECHNICAL DISCUSSION

Since RCA's fabrication experience with Mylar was limited and a relatively close schedule was required for model delivery, a fabrication specification (see Appendix) was prepared, outlining the requirements for the inflatable torus sail array. The specification was submitted to three vendors experienced in the fabrication of Mylar structures. None of the three prospective vendors could guarantee delivery of a leak-tight model; therefore, since the quality of workmanship was to be that normally expected for a laboratory development model, it was decided to fabricate the model at RCA.

Model fabrication was quite difficult at first. Mylar exhibits an excellent shape-retention memory and simple fabrication techniques were quickly proven fruitless. Efforts to develop a torus by bonding two flat sheets of Mylar with two concentric rings were soon discounted because of the relatively inelastic behavior of the material. An inflatable torus structure formed out of Mylar material requires initial fabrication as a torus, a property similar to forming metal. Because of the three dimensional curvature an unwrinkled torus composed of flat pieces of Mylar is extremely difficult to fabricate. Recourse was made to the segmented section fabrication technique which evolved in the process of building the model. This consists of making pie-shaped tube sections which are successively joined in a bead-type manner over a copper torus mandrel as shown in Figure 25. The tube sections are formed out of flat sheets of Mylar with the aid of an aluminum template. Radial and circumferential joints are bonded with Schjelbond thermoplastic strip adhesive tape.

Two prototype models were fabricated. The first torus model, shown in Figure 26, was made of 1/2 mil Mylar and was primarily used as an exploratory model to develop sealing and fabrication techniques. Pressurization of this model revealed good torus structural conformity. Gas leakage, however, primarily at the joints, required continuous pressurization to keep the model inflated. The second model was made of a Mylar-dacron scrim-Mylar lamination which simplified fabrication. All joints were double sealed to minimize leakage. Pressurization again revealed an inability to achieve good joint seals, thus corroborating the experience of vendors contacted to fabricate the model. Sample Mylar specimens were then sent to an ultrasonic bonding firm which uses a high frequency machine for sealing Mylar to Mylar. Sealing results of the tests were discouraging however, and further efforts in this direction were abandoned.

The following modifications were incorporated in a third model in an effort to prevent or minimize the leakage problem:

a. The diameter of the tube forming the torus was increased from 1-1/2 to 2-1/2 inches. This change reduced the pressure requirement for supporting the 3-foot-diameter torus dish.

b. The outer circumferential joint was eliminated by a new fabrication technique.

c. Shear-type adhesive joints were used to replace the pell-type joints previously used. This joint provides greater strength by using the full bonded area to carry the load.

d. Internal as well as external adhesive tape was used at all radial joints to provide circumferential continuity to the cemented sections.

Figure 25. Segmented-Section Technique for Forming A Mylar Torus

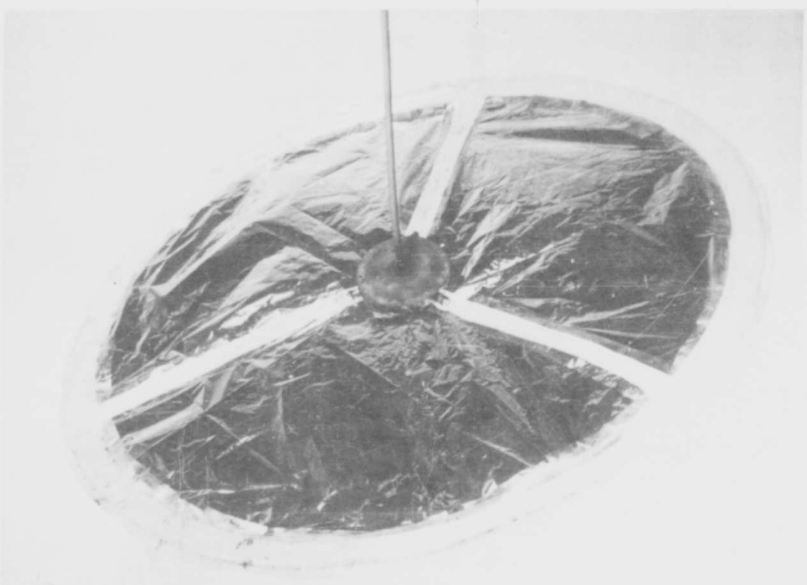

Figure 26. Inflated Torus-Sail Model

The resulting model, shown in Figure 27, has given the best performance to date. Repeated folding and unfolding during demonstration of the model has been found to have a deleterious effect on the adhesive sealing characteristics of the thermoplastic strip. This is attributed to the brittle nature of the adhesive. A stand for the model incorporates an epoxy glass dome, needle valve, and pressure container for demonstration purposes. A plastic dome will enclose the folded array to protect it during handling.

To surmount the leakage rate and 1-g sea-level difficulties, a mechanism was devised to support the torus sail when inflated. The mechanism is shown in Figure 28. Gas pressure is merely required to deploy the folded array. The support mechanism consists of six folding and twisting radial umbrella-type ribs and dacron cord spiderweb support. The rib support maintains the planar integrity of the model. Efforts to incorporate the rib support in the model were abandoned by mutual agreement between ASD representatives and RCA when it was decided not to mount the CdS cells to the model.

SUMMARY AND CONCLUSIONS REGARDING TORUS SAIL ARRAY

The major problem area in developing a full scale inflatable torus-sail solar cell array is to fabricate a leak-tight structure out of plastic film or metal foil. The ECHO I inflatable balloon satellite gives factual evidence of structural deformation due to the loss of internal pressure. Recent efforts to pressurize future balloons above the material elastic limit, as a method of shape retention, appear promising for a structure possessing isotropic stress distribution. Reliability of this method should a pressure loss occur in space is still questionable. Reliability can be further enhanced by incorporating a mechanical folding rib-type support, or cured foam pressurization technique, which would provide permanent rigidity for retention of the structural planar configuration. It is particularly advisable in applications where personnel safety is a design consideration, and it would obviate the need for continuous gas pressurization should micrometeorite bombardment and subsequent puncture occur. The weight penalty would be minor with a significant improvement in reliability.

B. TELESCOPING ARRAY

INTRODUCTION

Although the most promising array was considered to be the torus sail, a telescoping array also has many merits and was selected as the second model to be delivered. The area density of this array, not including the solar cells and wiring, but including the structure, sail and cover, is 0.09 lb/ft^2. This density is calculated for an array having an area of 100 ft^2. A drawing of a model of a telescoping array is shown in Figure 29.

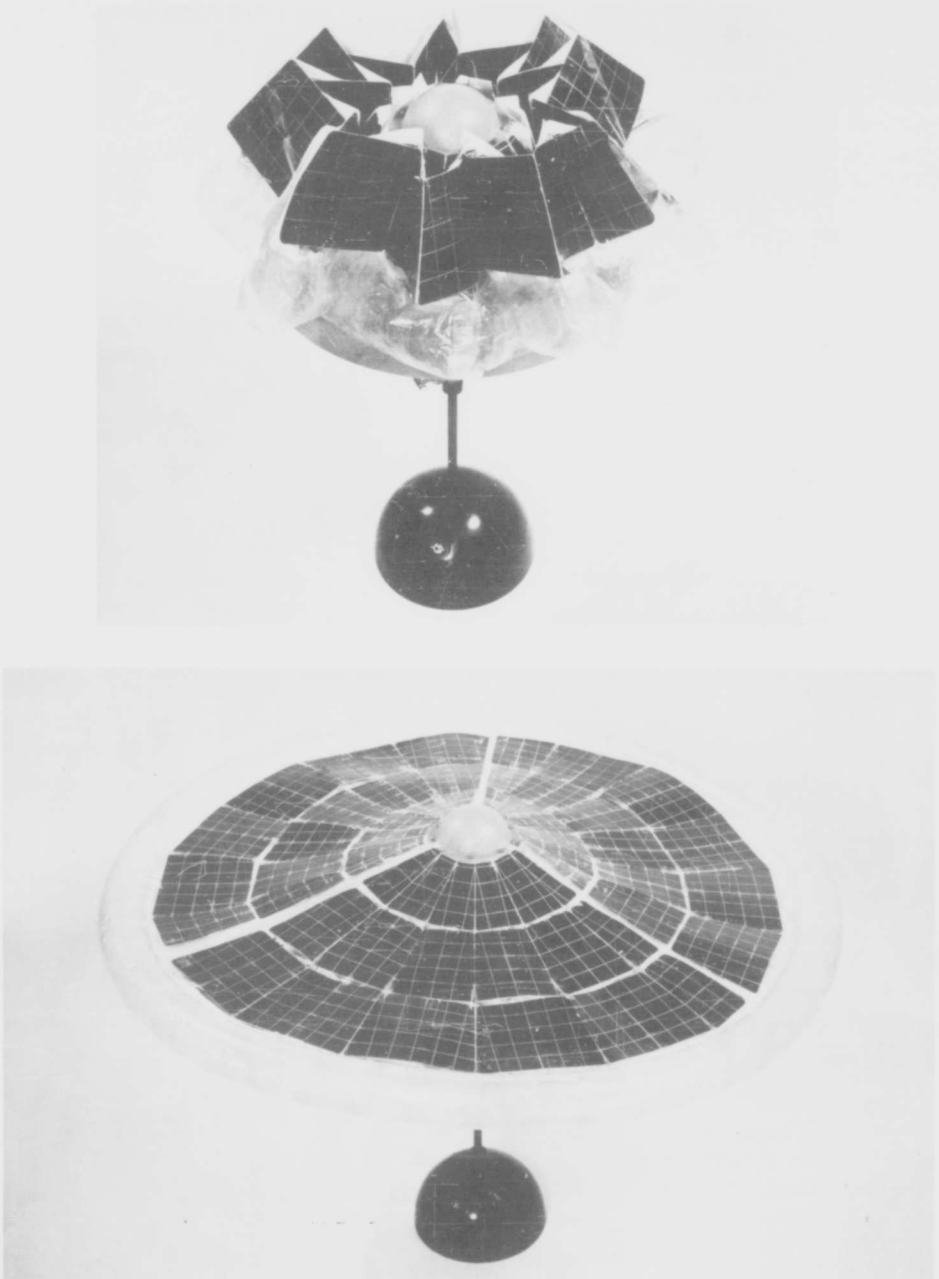

Figure 27. Torus-Sail Prototype Model

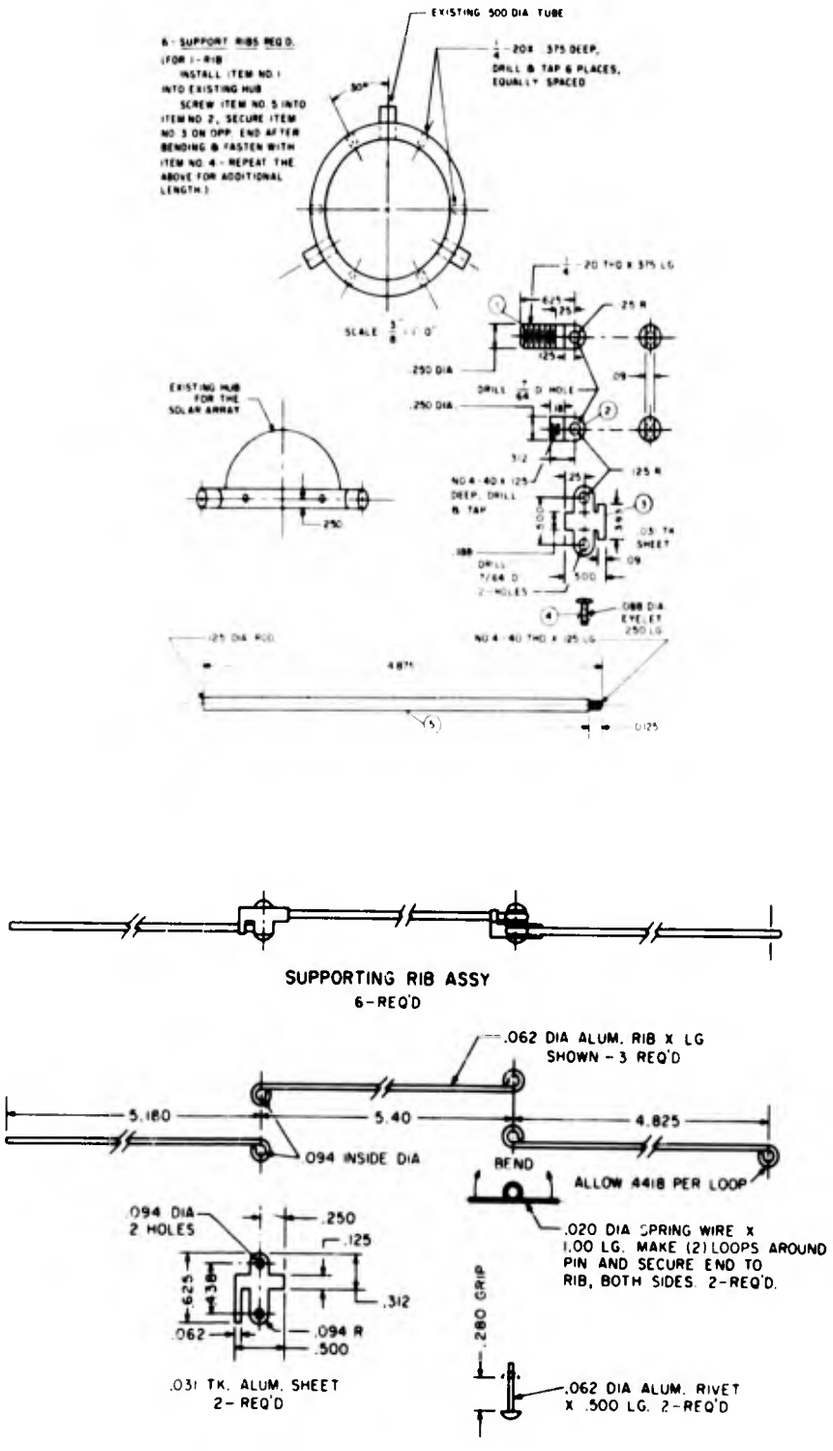

Figure 28. Torus-Sail Support Mechanism

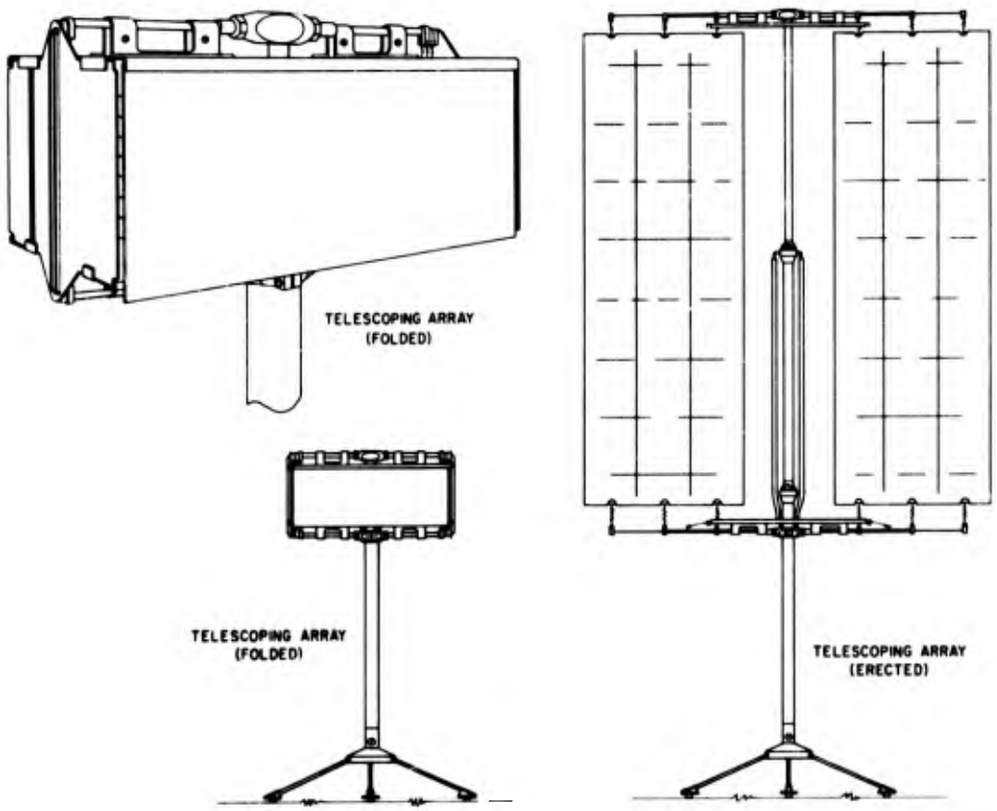

Figure 29. Telescoping Array

TECHNICAL DISCUSSION

1. GENERAL

Although inflatable arrays studied in this program exhibited lowest area densities, the problems of reliability of the erection system and of maintaining planar integrity warranted consideration of other array systems. Mechanical systems were evaluated and the telescoping array was found to meet most of the requirements.

2. OPERATION

The telescoping array requires a differential gas pressure of 20 $lb/in.^2$ acting on the telescoping members, which behave like pistons in a cylinder to achieve erection. Once a telescoping member is fully extended, it locks into place and no longer needs a differential pressure to stay erected.

The sequence of erection is most important. If the vertical members, which form the mast of the array, and the horizontal members should open simultaneously, the sail with solar-cell modules attached would be badly damaged. The vertical mast must open first. To achieve this sequence, the joints of the vertical mast act as stops, pistons, locking devices, and switches. The gas is not permitted to act on the horizontal members until the vertical mast is fully extended and locked in position.

When the vertical mast starts extending, the retainers on the protective cover are released, and the sides of the protective cover are opened by the force of torsion springs acting upon them. Padding is used to keep solar-cell modules from clattering on each other. This padding is ejected by the sail itself as it unfolds. A sequence of the deployment of the array is shown in Figure 30.

3. FABRICATION

a. Planar integrity.- The efficiency of a solar cell varies as its orientation with respect to the sun varies. If a cell is oriented so that its surface is normal, i.e., perpendicular, to the sun's rays impinging upon it, it is assumed to be 100 percent direction efficient. This efficiency is approximately proportional to the cosine of the angle between sun direction and the cell normal. In determining the allowable deviation of an array surface from flatness, two conditions were considered:

a. that of allowable loss in solar cell direction efficiency, and

b. that of the accuracy of the positioning device.

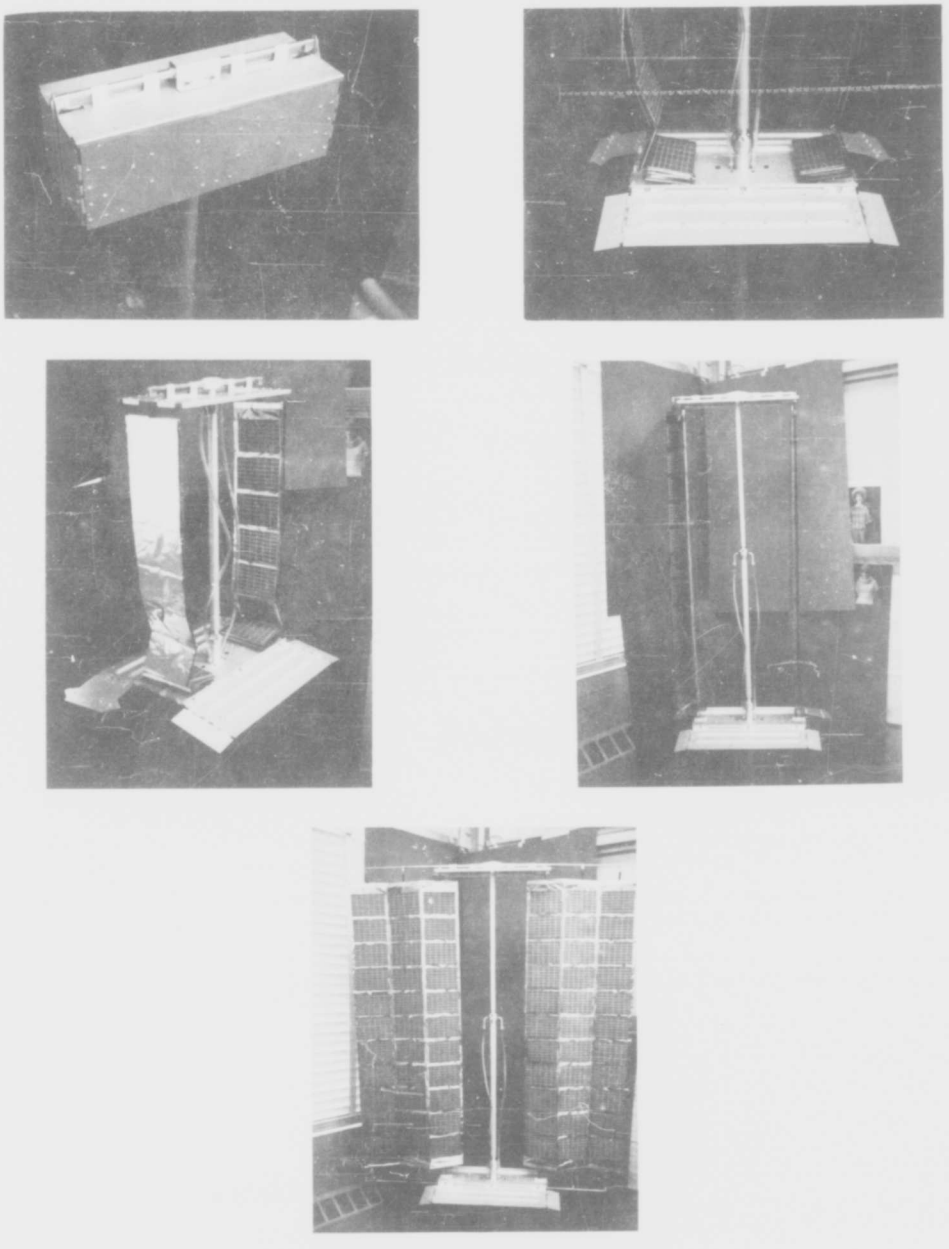

Figure 30. Sequence of Deployment of Telescoping Array

After approximately 50 foldings and deployments, the telescoping array sail was found to deviate somewhat from flatness as shown schematically in Figure 31. The linear deflection, d, was found to be approximately 1 inch. Calculations in this study have shown that such a deflection implies that the cell direction efficiency is at least 94 percent for an oriented system with a positioner of ±10 percent accuracy.

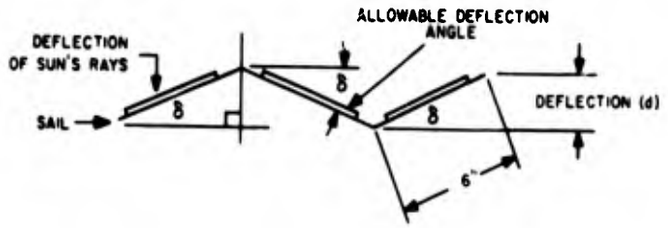

Figure 31. Deviation from Flatness of Telescoping Array after Repeated Operation

b. Materials.- The materials used are compatible with the space, storage, and handling environments for the lengths of time that they would be required to perform in a space environment. In general, the materials used are as follows:

1) Metals

a. Aluminum alloys. The alloys used are the higher strength aluminum alloys with a hard, clear, anodized finish applied to the surface.

b. Stainless steel. 18-8 composition stainless steels are used with a passivating dip for stainless steels applied to the surface.

2) Non-metals

a. A 0.0005-inch polyester film with an aluminized surface is used for the sail.

b. Poly-sulphide adhesives are used for bonding to the polyester film.

c. Anaerobic self-hardening polyester sealants are used as thread-locking agents.

d. Poly-urethane foams are used for padding.

e. Poly-vinyl chloride tubing is used for supplying gas to the erection mechanism (can be destroyed by environment after erection).

c. Construction

1) Erection system

The vertical mast sections are made of 0.062-inch wall aluminum tubing of 0.750, 1.000, and 1.250-inch outside diameters respectively. The end fittings are made of stainless steel which results in an increase in weight, but which reduces the friction factor of the sliding members by having dissimilar materials in contact with one another.

The horizontally telescoping tubes are made of 0.010-inch walled stainless steel tubing, which results in a lower weight than could be accomplished with .031-inch wall aluminum tubing.

2) Sail

The sail is suspended from hangers on the upper telescoping members by double-snap barrel swivels, and from the lower telescoping members by single-snap barrel swivels and extension springs. The springs keep the sail in tension and flat. The solar cell modules are fastened to the sail with a poly-sulphide adhesive.

3) The solar-cell module

Each module consists of 48 1 x 2-cm silicon solar cells. There are eight cells in a series string; six series strings are wired in parallel to comprise each module. Modules may be wired in parallel or in series, according to the requirements of the system. Figure 32 shows the interconnections of the cells.

4) The enclosure system

Aluminum sheet is used in the fabrication of the enclosure system. The system consists of a top wall attached to the upper horizontal telescope, a bottom wall attached to the lower horizontal telescope and, two long spring-loaded slides attached by hinges to the bottom wall. Two spring-loaded small 1/3 sides are attached to one of the long sides by hinges, and two spring-loaded small 2/3 sides with telescope stops are attached to the other long side by hinges.

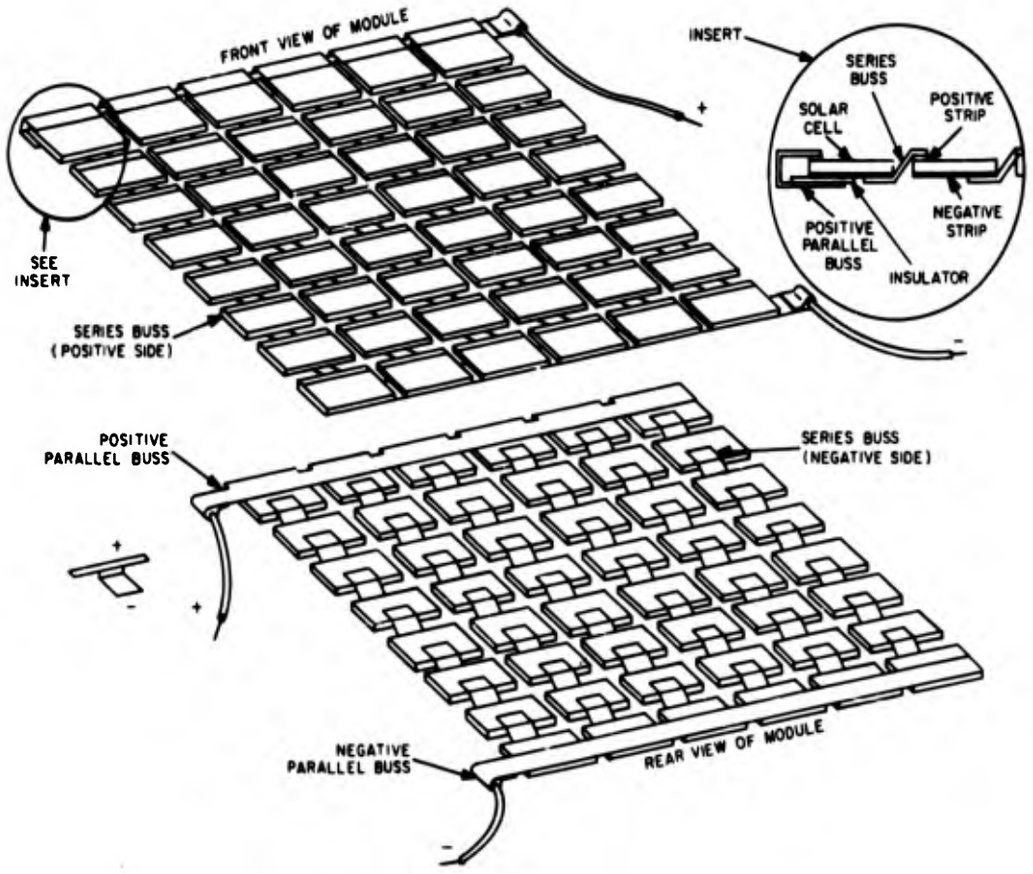

Figure 32. Solar Cell Interconnections

When in the stored position, the long sides are held in place by retaining strips on the upper wall, and the small sides are held in position by retaining slips in both the top and bottom walls. The small 2/3 sides have extensions on them which keep the horizontal telescopes from opening until the erection system is energized.

When the erection system is energized and the vertical tubes rise, the top wall rises with them, releasing the long sides and the tops of the short sides. Spring pressure causes the long sides to turn outward on their hinges (attached to the bottom wall). When the long sides are half open, the short sides, which are carried with them, are released from their retainers on the bottom wall. The small sides then open with respect to the long sides, also by spring pressure.

Twenty pounds/in.^{2} differential pressure is required to erect this array. This pressure can be supplied to fittings attached to the bottom of the vertical mast.

d. Tests.- The telescoping array has had approximately 50 consecutive successful erections at sea level, and two successful consecutive erections in the horizontal position in a vacuum of 10^{-4} to 10^{-5} mm Hg.

SUMMARY REGARDING TELESCOPING ARRAY

The telescoping array module simulates a highly reliable, optimized space solar-cell array. The area density of such a space array would be about 0.09 lb/ft^2. With this type of space array areas up to about 1000 square feet could be achieved.

The model as delivered demonstrates the salient mechanical features of the optimized array and, in addition, provides about 1 watt of electrical power when exposed to radiation equivalent to solar radiation.

V. TEST RESULTS

Near the latter stages of the fabrication phase period, ASD and RCA mutually agreed to omit portions of the contract requirements.

Included in this change were the following:

1. The CdS cells need not be wired or attached to the torus-sail structure.

2. Neither the torus-sail structure nor the telescoping-sail array need be environmentally tested.

As a result of this change, this technical report does not contain the test report prepared in accordance with Specification MIL-T-9107 nor the final design specification (MIL-S-6644)

TECHNICAL SUMMARY

Models of two types of solar cell arrays have been fabricated. One, the torus sail, is an array for space use that has extremely low structure (excluding cells) weight per unit area (less than .04 lb/ft^2); the other, the telescoping sail, is also an array of low weight per unit area (about .09 lb/ft^2), but in addition its mechanical characteristics make it insensitive to micrometeorite bombardment.

Development of thin film photovoltaic cells has been pursued to provide very lightweight cells for use with such arrays. Evaporated CdS cells have been fabricated in several sizes. A maximum efficiency of 4.5 percent has been attained for a cell of area 1.6 cm^2. In general, the present limitation in cell size arises from the high sheet resistance of the transparent conducting layer. The sheet resistance causes a decrease in efficiency with increased cell size. In addition, deterioration in efficiency occurs when the cells are exposed to the atmosphere for extended periods. This effect, of course, would not exist in a space environment. It is anticipated that the problems associated with high sheet resistance and efficiency deterioration caused by atmospheric effects will be reduced by further research and development during the remainder of this study.

Preliminary radiation damage studies showed that polycrystalline CdS cells are as good as, and probably better, than n-on-p silicon cells with respect to efficiency decrease after exposure to 0.8 Mev electrons. It should be noted that n-on-p cells have been found much more radiation resistant than standard p-on-n cells.

It has been demonstrated that a polycrystalline thin-film layer of CdS may be converted to a layer composed of larger crystals. The larger crystal layer offers the low weight associated with thin films and the possible potential for the high efficiency associated with the photovoltaic properties of large crystals of CdS.

This phase of the contract work has resulted in the fabrication of both thin film photovoltaic CdS cells and two solar-cell array models. During the work, the performance characteristics of the cells were improved to the point where the power-to-weight ratio was comparable to that of silicon cells. Further improvement in the fabrication of this thin film type of cell offers the possibility of obtaining power-to-weight ratios significantly higher than those of conventional silicon cells now in use. The remainder of the contract work will be devoted to exploiting this potential.

BIBLIOGRAPHY

1. Shirland, F. A., "Photovoltaic Cadmium Sulfide", ARL Technical Report, 60-293 (August, 1960) (AD-246547).

2. Gilles, J. M., and Van Cakenberghe, J., Nature, 182, 862 (1958).

3. Gilles, J. M., and Van Cakenberghe, J., Solid State Physics in Electronics and Telecommunications, 2, 900 (1960); Part 2, Semiconductors; Academic Press, Inc. (London).

4. Burke, J. E., and Turnbull, D., Progr. in Metal Phys., 3, 220 (1952).

5. Shallcross, F. V., and Dresner, J., private communication.

6. Beck, P. A., Holzworth, M. L., and Sperry, P., Trans. Am. Inst. min. (metall.) Engrs. 180, 163 (1949).

7. Seiwert, R., Ann. Physik, 6:241 (1949).

8. Woods, J., Brit. J. Appl. Phys., 11, 296 (1960).

9. Wysocki, J. J., "The Effect of Series Resistance on Photovoltaic Solar Energy Conversion", RCA Review No. 1, 22, 57-70 (March, 1961).

APPENDIX
FABRICATION SPECIFICATION
PROTOTYPE MODEL-INFLATABLE
SOLAR ARRAY

1. SCOPE

This specification covers the requirements for the fabrication of a torus and rib supported, three foot diameter inflatable solar array prototype model.

2. APPLICABLE DOCUMENTS

Inflatable Solar Array Prototype Model (Dwg. 1176851) forms a part of this specification. (See Figure 33.)

3. REQUIREMENTS

3.1. The inflatable solar array prototype model shall consist of a three foot diameter membrane which is attached at its outer perimeter to a 2-1/2 inch diameter torus.

3.2. Inflation shall be achieved through a central hub section mount which pressurizes the three radial support ribs and torus.

3.3. Material selected shall be capable of successfully withstanding environmental conditions of outer space (-50°C to +80°C, and high vacuum of 10^{-9} mm Hg). It shall also be capable of repetitive folding without tearing or loss of sealing, and tolerate the effects of impinging meteoric and ionized particles.

3.4. Close shape tolerance shall be held with uniform and concentric sections and bonded joints to preserve structural integrity and homogeneity.

3.5. Sealed joints shall be made with Schjeldahl Co. GT-100 resin or Schjelbond, GT-400 resin adhesive, or equivalent.

3.6. An operating life of 1 year minimum is required with 100 cycles of pressure and folding without tearing or leakage.

4. QUALITY ASSURANCE PROVISIONS

4.1. Certification of a 15 psig proof pressure test with no leakage required.

4.2. One sample prototype model representing the quantity to be furnished hereunder shall be tested by the vendor in accordance with his customary procedures. Such tests shall be witnessed by the buyer, if desired, and approved prior to manufacture of the total quantity.

4.3. Final Acceptance. Acceptance of prototype models furnished hereunder shall be at the buyers plant. The vendor shall guarantee against latent defects in materials and workmanship which may be discovered by the buyer.

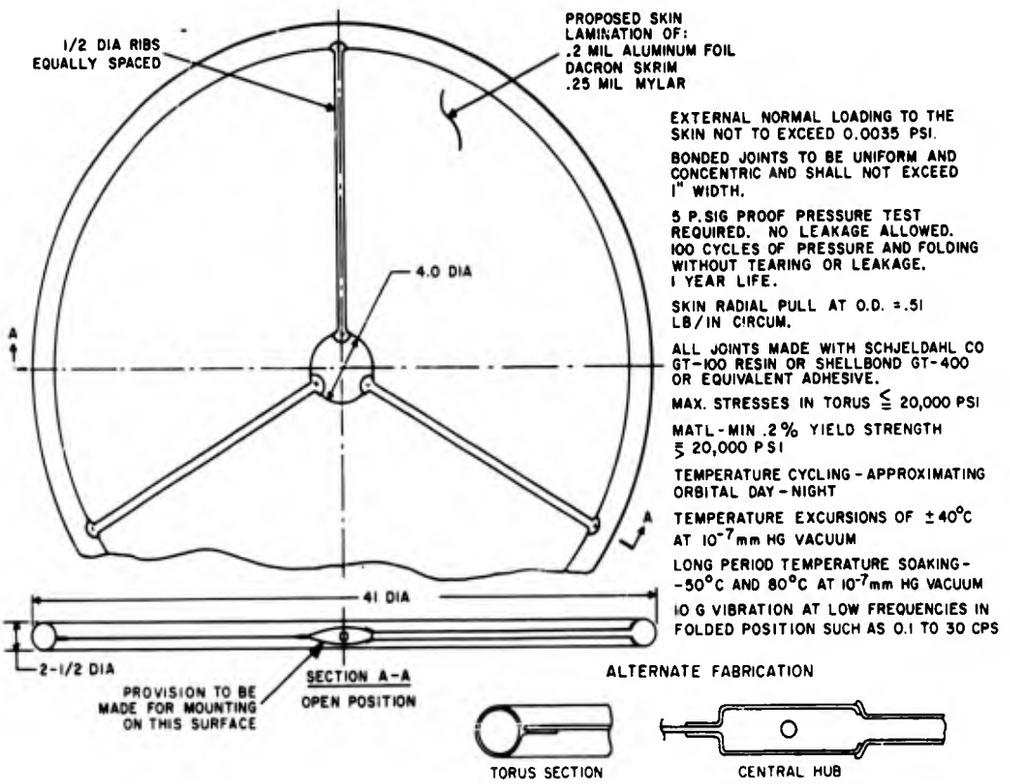

Figure 33. Inflatable Solar Array, Prototype Model, RCA Drawing No. 1176851

Aeronautical Systems Division, Wright-Patterson Air Force Base, Ohio. Rpt No. ASD-TR-61-11, Vol. II. SOLAR CELL ARRAY OPTIMIZATION. Feb 62, 85p, incl. illus; tables.

Unclassified Report

This report covers the fabrication and test of photovoltaic materials and design of solar-cell arrays for maximum conversion of solar energy with minimum weight. Evaporated layer cells with an efficiency of up to 4.5 percent over an area of 1.6 cm^2 were fabricated. Research on crystal layer conversion reduced the temperature for recrystallization from 500°C to 300°C. Two

(over)

models of solar-cell arrays to simulate a 100 ft^2 system were fabricated; the telescoping sail with a density of 0.075 lb/ft^2, and the inflatable torus sail with a density of 0.04 lb/ft^2. The maximum area of individual cells was increased by a factor of 27, thickness of substrate reduced by factor of 6, and weight reduced by factor of 7.

1. Solar Cells
2. Photovoltaic materials
3. Solar Energy Conversion

I. ASD Project 3145, Task 60959

II. Contract AF33(616)-7415

III. RCA, Astro-Electronics Div., Defense Electronic Products, Princeton, N. J.

IV. In ASTIA collection

V. Avail fr OTS:

Aeronautical Systems Division, Wright-Patterson Air Force Base, Ohio. Rpt No. ASD-TR-61-11, Vol. II. SOLAR CELL ARRAY OPTIMIZATION. Feb 62, 85p, incl. illus; tables.

Unclassified Report

This report covers the fabrication and test of photovoltaic materials and design of solar-cell arrays for maximum conversion of solar energy with minimum weight. Evaporated layer cells with an efficiency of up to 4.5 percent over an area of 1.6 cm^2 were fabricated. Research on crystal layer conversion reduced the temperature for recrystallization from 500°C to 300°C. Two

(over)

models of solar-cell arrays to simulate a 100 ft^2 system were fabricated; the telescoping sail with a density of 0.075 lb/ft^2, and the inflatable torus sail with a density of 0.04 lb/ft^2. The maximum area of individual cells was increased by a factor of 27, thickness of substrate reduced by factor of 6, and weight reduced by factor of 7.

1. Solar Cells
2. Photovoltaic materials
3. Solar Energy Conversion

I. ASD Project 3145, Task 60959

II. Contract AF33(616)-7415

III. RCA, Astro-Electronics Div., Defense Electronic Products, Princeton, N. J.

IV. In ASTIA collection

V. Avail fr OTS:

Aeronautical Systems Division, Wright-Patterson Air Force Base, Ohio. Rpt No. ASD-TR-61-11, Vol. II. SOLAR CELL ARRAY OPTIMIZATION. Feb 62, 85p, incl. illus; tables.

Unclassified Report

This report covers the fabrication and test of photovoltaic materials and design of solar-cell arrays for maximum conversion of solar energy with minimum weight. Evaporated layer cells with an efficiency of up to 4.5 percent over an area of 1.6 cm^2 were fabricated. Research on crystal layer conversion reduced the temperature for recrystallization from 500°C to 300°C. Two

(over)

models of solar-cell arrays to simulate a 100 ft^2 system were fabricated; the telescoping sail with a density of 0.075 lb/ft^2, and the inflatable torus sail with a density of 0.04 lb/ft^2. The maximum area of individual cells was increased by a factor of 27, thickness of substrate reduced by factor of 6, and weight reduced by factor of 7.

1. Solar Cells
2. Photovoltaic materials
3. Solar Energy Conversion

I. ASD Project 3145, Task 60959

II. Contract AF33(616)-7415

III. RCA, Astro-Electronics Div., Defense Electronic Products, Princeton, N. J.

IV. In ASTIA collection

V. Avail fr OTS:

Aeronautical Systems Division, Wright-Patterson Air Force Base, Ohio. Rpt No. ASD-TR-61-11, Vol. II. SOLAR CELL ARRAY OPTIMIZATION. Feb 62, 85p, incl. illus; tables.

Unclassified Report

This report covers the fabrication and test of photovoltaic materials and design of solar-cell arrays for maximum conversion of solar energy with minimum weight. Evaporated layer cells with an efficiency of up to 4.5 percent over an area of 1.6 cm^2 were fabricated. Research on crystal layer conversion reduced the temperature for recrystallization from 500°C to 300°C. Two

(over)

models of solar-cell arrays to simulate a 100 ft^2 system were fabricated; the telescoping sail with a density of 0.075 lb/ft^2, and the inflatable torus sail with a density of 0.04 lb/ft^2. The maximum area of individual cells was increased by a factor of 27, thickness of substrate reduced by factor of 6, and weight reduced by factor of 7.

1. Solar Cells
2. Photovoltaic materials
3. Solar Energy Conversion

I. ASD Project 3145, Task 60959

II. Contract AF33(616)-7415

III. RCA, Astro-Electronics Div., Defense Electronic Products, Princeton, N. J.

IV. In ASTIA collection

V. Avail fr OTS:

UNCLASSIFIED